



MINISTRY OF AVIATION

AERONAUTICAL RESEARCH COUNCIL
REPORTS AND MEMORANDA

Bending Flutter of Unstalled Cascade Blades at Finite Deflection

By D. S. WHITEHEAD, M.A., Ph.D., A.M.I.Mech.E., A.F.R.Ae.S.,
UNIVERSITY OF CAMBRIDGE, ENGINEERING LABORATORY

LONDON: HER MAJESTY'S STATIONERY OFFICE

1965

PRICE 15s. 6d. NET

Bending Flutter of Unstalled Cascade Blades at Finite Deflection

By D. S. WHITEHEAD, M.A., Ph.D., A.M.I.Mech.E., A.F.R.Ae.S.,

UNIVERSITY OF CAMBRIDGE, ENGINEERING LABORATORY

*Reports and Memoranda No. 3386**

October, 1962

Summary.

This report gives a method of calculating the conditions under which a cascade of unstalled blades will flutter in their bending mode. The blades are assumed to be flat plates and the flow is assumed to be two-dimensional. It is found that, when there is deflection of the steady flow through the cascade, bending flutter can occur in which there is a phase difference between the motion of one blade and its neighbours. The flutter boundaries for a range of cascades have been calculated on a digital computer and are presented. For turbine cascades these boundaries are not far from typical operating conditions in gas turbines and this may be why blades in the low pressure end of steam turbines have been found to require lacing wires. Comparisons are made with earlier theories due to Sohngen and Shioiri.

1. *Introduction.*

In the development of axial-flow compressors and turbines, blade vibration has been one of the most difficult problems encountered. Due to the large mass of the blades compared with the mass of the gas in their immediate vicinity, aerodynamic coupling between the various modes of vibration of each blade is not significant, and each blade can be considered as though it vibrated in a single degree of freedom which may be either bending or torsion. This report is concerned with calculating the conditions under which self-excited bending vibration of the blades can occur. The blades will be considered to be unstalled, since an analytic solution of the stalled flow does not appear to be feasible at the present time. The theory may therefore be expected to be more applicable to turbine blades, which seldom run stalled, than to compressor blades, which are often stalled at off-design conditions and for which stall flutter is likely to be the more serious limitation.

There is a considerable amount of experimental evidence that bending flutter of unstalled cascade blades can occur. Shannon¹ has reported a pure bending vibration in a compressor cascade which gave large stresses at incidences below the stalling incidence, but this case may have been a compressibility effect.

* Replaces A.R.C. 24 059.

Bellenot and d'Epina² have reported bending flutter over a range of incidence in which the blades would not be expected to be stalled. Shioiri⁷ has made the most complete investigation of unstalled bending flutter, using a cascade in which the first and last of a group of blades which could vibrate were mechanically coupled together, so as to simulate the effect of an infinite cascade. Unstalled bending flutter has also been observed by Leclerc⁸ and by Skarecky⁵. In all cases the flutter occurs with a phase difference between one blade and the next, and Bellenot and d'Epina² report that if the blades are connected together with a wire, so that all blades must vibrate in phase, then the flutter does not occur.

In a large proportion of the theoretical work done on the vibration of unstalled cascade blades it has been assumed that the mean deflection of the air flowing through the cascade is small. These calculations show that bending vibration is always damped (*see*, for instance, Ref. 11) although torsional flutter can occur⁴. However, Molyneux¹⁰ has shown that three-dimensional effects can give rise to bending flutter in a helicopter rotor under zero deflection conditions. In order to account for bending flutter in two-dimensional flow it is necessary to allow for the steady deflection. The first theory to do this was given by Bellenot and d'Epina², and they gave the following qualitative physical explanation of the effect.

Referring to Fig. 1, suppose that the blade numbered 0 can vibrate, but all the others are fixed. Then if blade 0 was removed, owing to the steady deflection through the cascade there will be a velocity gradient in the space between blades 1 and -1. The velocity will be high near the convex surface of blade -1 and low near the concave surface of blade 1. Therefore, when blade 0 is displaced upwards due to its vibration it moves into a region of lower velocity and would therefore be expected to produce less lift. Conversely, when it is displaced downwards the lift would be increased. If the flow were steady this would be equivalent to an increase in the spring force acting on the blade. But in fact the flow is not steady, and the circulation round the blade can only change slowly by means of vorticity shed from the trailing edge. Therefore, when the blade is in its mean position and is moving upwards it still retains some of its extra lift generated when it was displaced downwards. This force will therefore do work on the vibration and the system will tend to be unstable.

This explanation is of course highly oversimplified, but it does show that the essential ingredients of any theory are mean deflection of the flow, relative movement of the blades, and phase lag due to the rate at which circulation can be shed from the trailing edge. Bellenot and d'Epina² considered that the effect of the neighbouring blades was equivalent to a rotation of the blade under consideration, and they then used ordinary single aerofoil theory to give results which agreed quite well with their experiments.

This type of approach has been improved by Shioiri⁶ who assumed that all the blades vibrated and all the blades except the blade under consideration could be represented by point vortices, and then considered their effects on the centre blade. This produced results in good agreement with his experiments. A different type of theory has been given by Sohngen³, using the approximation that the vorticity on the blades can be spread out in a direction along the cascade so as to give a smooth continuous function for the vorticity variation in this direction. This theory is accurate when the spacing of the blades is small and the phase difference between one blade and the next is also small. A theory⁹ has been given by the author which uses the concept of replacing the cascade by an actuator disc. This theory should hold when the phase angle between adjacent blades and the frequency of vibration are both small, but it has been found that certain terms were omitted in the

original analysis which are important in the application of that theory to the case when there is finite deflection in the cascade, although the other cases treated are unaffected. This theory will be corrected in this report, and it is then found that the actuator-disc theory reduces to a special case of Sohngen's theory³.

The assumptions made in the above theories appear to be very restrictive, and it was therefore thought to be worthwhile to extend a previous analysis¹¹ for the zero-deflection flow to the case with finite deflection of the flow. The assumptions made in the present report are as follows:

- (a) The system considered is two-dimensional, so that the bending modes of actual blades are represented by a translational motion of the two-dimensional aerofoils. Only translational motion perpendicular to the chord line has been considered.
- (b) The fluid has been assumed to be incompressible and inviscid.
- (c) It is assumed that the blades do not stall, so that the flow always follows the blade surface.
- (d) Effects due to blade camber and thickness are neglected, so that the blades are assumed to be flat plates.
- (e) The amplitude of vibration is assumed to be small, so that the theory becomes linear, and any two types of vibration can be superposed to give a third type of vibration.
- (f) It is assumed that all blades vibrate with the same amplitude and with a constant phase angle between one blade and the next. This involves no loss of generality, since any required motion of the blades can be obtained by superposing solutions of the type considered. If all the blades are mechanically identical, then the flutter modes are of the type considered.
- (g) The positioning of the vorticity in the wakes of the blades will not be quite correct, since the wakes will be assumed to lie in straight lines in line with the blades and to be convected downstream at the mean flow velocity, the effect of deviation being neglected in this respect. The error may be expected to be small unless the blades are very widely spaced.

2. General Theory.

2.1. Summary of Method of Calculation.

Since the calculation is rather lengthy, the overall method to be used will first be summarised. It is supposed that the blades are vibrating with given amplitude and phase relationships and the object is to calculate the aerodynamic forces acting on the blades. Since the blades are flat plates, both the blades and their wakes may be replaced by vortex sheets. The strength of the vorticity on the blades has two components, a steady component ζ , and a fluctuating component γ . γ is assumed to be small but ζ is not small. ζ will induce steady velocities over the plane and γ will induce fluctuating velocities. But when the blades vibrate they carry their circulation with them. There are therefore further induced velocities to be considered due to the movement of the ζ vorticity which are of first order. The velocities induced by the movement of the γ vorticity are of second order and therefore negligible. ζ and γ must be arranged so that the correct upwash velocities are induced at the blades. When ζ and γ have been found the forces on the blades can be calculated, but this requires a knowledge of the velocities induced parallel to the chord, so that the velocities induced both parallel and perpendicular to the chord are required. Finally it can be determined whether the forces are such as to give aerodynamic damping or excitation (flutter). The first step is therefore to obtain expressions for the induced velocities. The notation used is illustrated in Fig. 2.

2.2. Velocities Induced by a Row of Unsteady Vortices.

Consider the row of vortices with the spacing, stagger angle and phasing of the cascade as shown in Fig. 3. One vortex of strength $\Gamma_m e^{i\omega t}$ at (x_m, y_m) induces at a point $(\eta, 0)$ velocities given by

$$u e^{i\omega t} = \frac{\Gamma_m}{2\pi} \frac{y_m}{(\eta - x_m)^2 + y_m^2} e^{i\omega t},$$

$$v e^{i\omega t} = \frac{\Gamma_m}{2\pi} \frac{(\eta - x_m)}{(\eta - x_m)^2 + y_m^2} e^{i\omega t}.$$

If the centre vortex at $(x, 0)$ has strength Γ_0 then the strength of a vortex on the m th blade or in its wake is given by

$$\Gamma_m e^{i\omega t} = \Gamma_0 e^{i(\omega t + m\beta)}$$

since on the m th blade everything will be advanced in phase by an angle $m\beta$. The position of this vortex is given by

$$x_m = x + ms \sin \xi,$$

$$y_m = ms \cos \xi.$$

The velocities induced by the complete row of vortices are therefore given by

$$u = \frac{\Gamma_0}{2\pi} \sum_{m=-\infty}^{+\infty} \frac{e^{im\beta} ms \cos \xi}{(\eta - x - ms \sin \xi)^2 + (ms \cos \xi)^2},$$

$$v = \frac{\Gamma_0}{2\pi} \sum_{m=-\infty}^{+\infty} \frac{e^{im\beta} (\eta - x - ms \sin \xi)}{(\eta - x - ms \sin \xi)^2 + (ms \cos \xi)^2}.$$

These expressions may be written:

$$u = \frac{\Gamma_0}{c} U \left(\frac{\eta}{c} - \frac{x}{c} \right), \quad (1)$$

$$v = \frac{\Gamma_0}{c} V \left(\frac{\eta}{c} - \frac{x}{c} \right), \quad (2)$$

where $U(z)$ and $V(z)$ are functions of $z = (\eta - x)/c$ given by

$$U(z) = \frac{1}{4\pi} \frac{c}{s} \{e^{-i\xi} f(\chi) + e^{i\xi} f(\bar{\chi})\}, \quad (3)$$

$$V(z) = \frac{1}{4\pi i} \frac{c}{s} \{e^{-i\xi} f(\chi) - e^{i\xi} f(\bar{\chi})\}, \quad (4)$$

and

$$\chi = -iz \frac{c}{s} e^{-i\xi}, \quad (5)$$

$$\bar{\chi} = iz \frac{c}{s} e^{i\xi}, \quad (\text{complex conjugate of } \chi) \quad (6)$$

and

$$f(\chi) = \sum_{m=-\infty}^{+\infty} \frac{e^{im\beta}}{\chi + m}. \quad (7)$$

This series can be summed by standard methods. The result for $0 < \beta < 2\pi$ is

$$f(\chi) = \pi e^{i(\pi - \beta)\chi} \operatorname{cosec} \pi \chi. \quad (8)$$

However, when $\beta = 0$ then the summation gives

$$f(\chi) = \pi \cot \pi \chi. \quad (9)$$

This differs from the result of putting $\beta = 0$ in equation (8). However, it is found that the effect on the $U(z)$ and $V(z)$ functions of using equation (8) with $\beta = 0$ instead of equation (9) is to add constant terms (independent of z) to these functions. This is equivalent to superposing a constant velocity over the whole field. Since it will be found that it is only the difference between the velocity induced at any point and the velocity induced far upstream which is of significance, this constant has no effect, and equation (8) will be used for the $\beta = 0$ case as well as for $0 < \beta < 2\pi$.

2.3. Velocity Induced by Displacement of a Row of Steady Vortices.

Consider a row of vortices with the spacing and stagger angle of the cascade in question, and each with a steady circulation Γ . The m th vortex is displaced upwards by a small distance h_m , as shown in Fig. 4, so that its co-ordinates are given by

$$\begin{aligned} x_m &= x + ms \sin \xi, \\ y_m &= h_m + ms \cos \xi. \end{aligned}$$

If h_0 is the displacement of the reference blade, then the velocities induced at the point (η, h_0) on the reference blade or in its wake are then given by

$$\frac{\Gamma}{2\pi} \frac{(y_m - h_0)}{(\eta - x_m)^2 + (y_m - h_0)^2} = \frac{\Gamma}{4\pi i} \left\{ \frac{-1}{(\eta - x_m) + i(y_m - h_0)} + \frac{1}{(\eta - x_m) - i(y_m - h_0)} \right\},$$

and

$$\frac{\Gamma}{2\pi} \frac{(\eta - x_m)}{(\eta - x_m)^2 + (y_m - h_0)^2} = \frac{\Gamma}{4\pi} \left\{ \frac{1}{(\eta - x_m) + i(y_m - h_0)} + \frac{1}{(\eta - x_m) - i(y_m - h_0)} \right\}.$$

Since the displacements are small these terms can be expanded by Taylor's theorem. For instance

$$\begin{aligned} \frac{1}{(\eta - x_m) + i(y_m - h_0)} &= \frac{1}{\eta - x - ms \sin \xi + i(h_m - h_0)} \\ &= \frac{1}{\eta - x - ms \sin \xi + i ms \cos \xi} - \frac{i(h_m - h_0)}{(\eta - x - ms \sin \xi + i ms \cos \xi)^2}. \end{aligned}$$

The first term gives the steady component of the induced velocity, and has already been considered, since it is a special case of the previous section. The second term gives the first-order fluctuating component due to the displacement. These velocities are

$$\begin{aligned} u e^{i\omega t} &= \frac{\Gamma(h_m - h_0)}{4\pi} \left\{ \frac{1}{(\eta - x - ms \sin \xi + i ms \cos \xi)^2} + \frac{1}{(\eta - x - ms \sin \xi - i ms \cos \xi)^2} \right\} \\ v e^{i\omega t} &= \frac{\Gamma(h_m - h_0)}{4\pi i} \left\{ \frac{1}{(\eta - x - ms \sin \xi + i ms \cos \xi)^2} - \frac{1}{(\eta - x - ms \sin \xi - i ms \cos \xi)^2} \right\}. \end{aligned}$$

Due to the phase relationship assumed for the cascade

$$h_m = h_0 e^{im\beta}.$$

Also it will be convenient to work in terms of the velocity of the reference blade, $qe^{i\omega t}$, instead of its displacement h_0 . Then

$$qe^{i\omega t} = \frac{d}{dt}(h_0) = i\omega h_0 = i\lambda U h_0/c$$

where λ is the frequency parameter ($\lambda = \omega c/U$) and U is the mainstream velocity. This gives

$$(h_m - h_0) = \frac{qc}{i\lambda U} (e^{im\beta} - 1)e^{i\omega t}.$$

Summing the result for all the vortices, the expressions for the induced velocities may be written as follows:

$$u = \frac{\Gamma q}{Uc} M \left(\frac{\eta}{c} - \frac{x}{c} \right), \quad (10)$$

$$v = \frac{\Gamma q}{Uc} N \left(\frac{\eta}{c} - \frac{x}{c} \right), \quad (11)$$

where $M(z)$ and $N(z)$ are functions given by

$$M(z) = \frac{i}{4\pi\lambda} \left(\frac{c}{s} \right)^2 \{e^{-2i\xi} g(\chi) + e^{2i\xi} g(\bar{\chi})\}, \quad (12)$$

$$N(z) = \frac{1}{4\pi\lambda} \left(\frac{c}{s} \right)^2 \{e^{-2i\xi} g(\chi) - e^{2i\xi} g(\bar{\chi})\}, \quad (13)$$

where χ is given by equation (5) and $g(\chi)$ is given by

$$g(\chi) = \sum_{m=-\infty}^{+\infty} \frac{e^{im\beta} - 1}{(\chi + m)^2}. \quad (14)$$

This series can be summed, either by differentiating equations (7) and (8) with respect to χ , or by contour integration methods. The result is

$$g(\chi) = \pi^2 \operatorname{cosec}^2 \pi \chi \left\{ \left(1 - \frac{\beta}{2\pi} \right) e^{-i\beta\chi} + \frac{\beta}{2\pi} e^{i(2\pi-\beta)\chi} - 1 \right\}. \quad (15)$$

This result holds for the range $0 \leq \beta \leq 2\pi$, and it will be noted that it gives $g = 0$ when $\beta = 0$ or 2π , which is obviously correct since there is then no relative displacement of the blades.

These equations give the required results for the induced velocities.

2.4. Calculation of Steady Vorticity.

The steady flow through the cascade consists of a uniform velocity U parallel to the blades together with the velocities induced by the steady vorticity on the blades. The net result is shown in Fig. 2, where the components of the velocity far upstream are shown as U_1 and τU , and similarly U_2 and $\tau_2 U$ far downstream. By continuity

$$U_1 \cos \xi - \tau U \sin \xi = U_2 \cos \xi - \tau_2 U \sin \xi = U \cos \xi$$

therefore

$$U_1 = U(1 + \tau \tan \xi),$$

and

$$U_2 = U(1 + \tau_2 \tan \xi).$$

The air inlet angle relative to the normal to the cascade is then given by

$$\tan \alpha_1 = (U_1 \sin \xi + \tau U \cos \xi) / U \cos \xi,$$

or

$$\tan \alpha_1 = \tan \xi + \tau \sec^2 \xi. \quad (16)$$

Similarly

$$\tan \alpha_2 = \tan \xi + \tau_2 \sec^2 \xi. \quad (17)$$

It will be convenient to use τ rather than α_1 as a measure of the incidence of the steady flow. Also, since the eventual object is to calculate the incidence at which flutter will occur, τ will be regarded as an unknown variable.

Now consider the velocities induced by the steady vorticity ζ . The steady velocities at $(\eta, 0)$ are

$$u = U + \int_0^c \{U_0(\eta-x) + k_u\} \zeta dx, \quad (18)$$

$$v = \int_0^c \{V_0(\eta-x) + k_v\} \zeta dx, \quad (19)$$

where $U_0(z)$ and $V_0(z)$ are the functions given by equations (3) and (4) when β is put equal to zero. These equations satisfy the conditions $u = U$ and $v = 0$ when $\zeta = 0$. The constants k_u and k_v must be added to the $U_0(z)$ and $V_0(z)$ functions to allow for the indeterminate constant in these functions which corresponds to a uniform velocity over the whole field. $V(z)$ behaves like $1/z$ when z is small, so that it is the principal value of the integral in equation (19) which is required.

Applying these equations far upstream gives

$$U(1 + \tau \tan \xi) = U + \int_0^c \{U_0(-\infty) + k_u\} \zeta dx, \quad (20)$$

$$\tau U = \int_0^c \{V_0(-\infty) + k_v\} \zeta dx. \quad (21)$$

Eliminating k_u and k_v from equations (18), (19), (20) and (21),

$$u = U(1 + \tau \tan \xi) + \int_0^c \{U_0(\eta-x) - U_0(-\infty)\} \zeta dx, \quad (22)$$

$$v = \tau U + \int_0^c \{V_0(\eta-x) - V_0(-\infty)\} \zeta dx. \quad (23)$$

Now on the blades the induced upwash velocity must be zero. So putting $v = 0$ in equation (23)

$$\int_0^c \{V_0(\eta-x) - V_0(-\infty)\} \zeta dx = -\tau U \text{ for } 0 < \eta < c.$$

This is an integral equation which determines ζ . Since ζ is proportional to τ it is convenient to write

$$\zeta = -\tau U \zeta_0 \quad (24)$$

where ζ_0 is the solution of the integral equation

$$\int_0^c \{V_0(\eta-x) - V_0(-\infty)\} \zeta_0 dx = 1 \text{ for } 0 < \eta < c. \quad (25)$$

This equation has to be solved subject to the Joukowski condition at the trailing edge, which means that ζ_0 must be finite when $x = 0$.

Once ζ_0 has been found, the chordwise velocities along the blades are given by equation (22) as

$$u = U + \tau U \left[\tan \xi - \int_0^c \{U_0(\eta - x) - U_0(-\infty)\} \zeta_0 dx \right]. \quad (26)$$

Since τ is being regarded as an unknown variable, it is convenient to write this as

$$u = U + \tau U u_0, \quad (27)$$

where

$$u_0 = \tan \xi - \int_0^c \{U_0(\eta - x) - U_0(-\infty)\} \zeta_0 dx. \quad (28)$$

In this report the downstream deviation effects will be neglected. The magnitude of the effect may be calculated by applying equation (23) far downstream where $v = \tau_2 U$, giving

$$\frac{\tau_2}{\tau} = 1 - \{V_0(+\infty) - V_0(-\infty)\} \int_0^c \zeta_0 dx. \quad (29)$$

α_2 may then be obtained from equation (17).

2.5. Free and Bound Vorticity.

In the zero-mean-deflection calculation it has been found convenient to divide the unsteady vorticity into two components, a bound vorticity and a free vorticity. The free vorticity is always being washed downstream at the mainstream velocity U , and the bound vorticity is zero in the wake. This division is necessary in order to handle a singularity which otherwise occurs at the trailing edge. A similar division will be made in the present calculation, but the free vorticity will not be a true free vorticity, since it will be defined on the basis that it is always being washed downstream at the velocity U , and not at the steady chordwise velocity given by equation (26). The relationship between γ (the bound vorticity) and ϵ (the free vorticity) will then be independent of τ . In the wake it will be assumed that the term proportional to τ in equation (26) is negligible, so that ϵ is here assumed to be a true free vorticity and γ is assumed to be zero.

The relationship between ϵ and γ is then exactly the same as in the zero-deflection calculation, but the derivation will be briefly repeated for the sake of completeness.

Consider an element of bound vorticity, $\gamma dx e^{i\omega t}$, at the point $(x, 0)$ on the reference blade. During a small time interval δt the strength of this element of bound vorticity changes by an amount

$$\gamma dx e^{i\omega t} i\omega \delta t.$$

This is equal in magnitude and opposite in sign to the free vorticity created in the time interval δt . Also during this time interval the free vorticity is assumed to move downstream a distance $U \delta t$. Hence the strength of the sheet of free vorticity at a point just behind the element of bound vorticity at $(x, 0)$ is given by

$$-\frac{\gamma dx e^{i\omega t} i\omega \delta t}{U \delta t} = -\frac{i\omega}{U} \gamma dx e^{i\omega t}.$$

Since the free vorticity is being continually washed downstream at a velocity U , the free vorticity at a point $(x_1, 0)$ farther downstream must be given by an expression of the form

$$\epsilon e^{i\omega t} = \text{constant } e^{i\omega(t - x_1/U)}.$$

Determining the constant from the previous considerations, writing $\lambda = \omega c/U$, and measuring distances in units of chordal length so that $c = 1$, gives

$$\epsilon = -i\lambda e^{i\lambda(x-x_1)}\gamma dx. \quad (30)$$

The total free vorticity at $(x_1, 0)$ is obtained by summing up the contributions from all the elements of bound vorticity from $x = 0$ to $x = x_1$. This gives

$$\epsilon = -i\lambda \int_0^{x_1} e^{i\lambda(x-x_1)}\gamma dx. \quad (31)$$

If this expression is multiplied by $e^{i\omega x_1/U}$, differentiated with respect to x_1 , and then written with x as the independent variable, the following differential relationship is obtained:

$$\frac{d\epsilon}{dx} + i\lambda(\gamma + \epsilon) = 0. \quad (32)$$

2.6. Velocity Induced by Vorticity on the Blade and in its Wake.

The velocities induced at a point $(\eta, 0)$ by an element of bound vorticity $\gamma dx e^{i\omega t}$ at $(x, 0)$ on the reference blade and corresponding elements on the other blades are given by

$$u(\eta) = \gamma(x) dx U(\eta - x), \quad (33)$$

$$v(\eta) = \gamma(x) dx V(\eta - x). \quad (34)$$

Associated with this bound vorticity is the free vorticity given by equation (30), which induces velocities given by

$$u(\eta) = \int_x^\infty \epsilon(x_1) U(\eta - x_1) dx_1, \quad (35)$$

$$v(\eta) = \int_x^\infty \epsilon(x_1) V(\eta - x_1) dx_1, \quad (36)$$

where the total effect is obtained by integrating over all the elements of free vorticity from x to infinity. Special consideration of the case $\beta = 0$ is required since for this case $U(z)$ and $V(z)$ do not tend to zero as $z \rightarrow -\infty$ and the above integrals do not converge but oscillate. To resolve this it is necessary to note that, assuming the system was started from rest, the total circulation due to each element of bound vorticity and its associated free vorticity is zero, so that

$$\gamma dx + \int_x^\infty \epsilon(x_1) dx_1 = 0.$$

If this equation is multiplied by the constant $U(-\infty)$ and subtracted from the sum of equations (33) and (35) there results

$$u(\eta) = \{U(\eta - x) - U(-\infty)\}\gamma dx + \int_x^\infty \epsilon(x_1)\{U(\eta - x_1) - U(-\infty)\} dx_1,$$

and similarly,

$$v(\eta) = \{V(\eta - x) - V(-\infty)\}\gamma dx + \int_x^\infty \epsilon(x_1)\{V(\eta - x_1) - V(-\infty)\} dx_1.$$

These integrals will now always converge at the top limit.

Substituting for ϵ from equation (30) and replacing x_1 by $z_1 = \eta - x_1$ gives

$$u(\eta) = \left[U(\eta - x) - U(-\infty) + i\lambda \int_{\eta-x}^{-\infty} e^{i\lambda(x-\eta+z_1)} \{U(z_1) - U(-\infty)\} dz_1 \right] \gamma dx,$$

$$v(\eta) = \left[V(\eta - x) - V(-\infty) + i\lambda \int_{\eta-x}^{-\infty} e^{i\lambda(x-\eta+z_1)} \{V(z_1) - V(-\infty)\} dz_1 \right] \gamma dx.$$

These equations can be written

$$u(\eta) = J(\eta - x)\gamma(x) dx, \quad (37)$$

$$v(\eta) = K(\eta - x)\gamma(x) dx, \quad (38)$$

where

$$J(z) = U(z) - U(-\infty) + i\lambda e^{-i\lambda z} \int_z^{-\infty} e^{i\lambda z_1} \{U(z_1) - U(-\infty)\} dz_1, \quad (39)$$

$$K(z) = V(z) - V(-\infty) + i\lambda e^{-i\lambda z} \int_z^{-\infty} e^{i\lambda z_1} \{V(z_1) - V(-\infty)\} dz_1. \quad (40)$$

Integrating equations (37) and (38) to give the velocities induced by all the elements of bound vorticity along the blade chords gives

$$u(\eta) = \int_0^1 J(\eta - x)\gamma(x) dx, \quad (41)$$

$$v(\eta) = \int_0^1 K(\eta - x)\gamma(x) dx. \quad (42)$$

Since $K(z)$ is infinite when $z = 0$ it is the principal value of this last integral which is required.

In the numerical evaluation of the $K(z)$ function two difficulties arise. One is the infinite limit on the integral and the other is the singularity in $V(z)$ which behaves like $1/2\pi z$ when z is small. It is shown in Ref. 11 that the $K(z)$ function is given by

$$K(z) = V(z) + i\lambda e^{-i\lambda z} \left[\int_z^{-1} \left\{ e^{i\lambda z_1} V(z_1) - \frac{1}{2\pi z_1} \right\} dz_1 - \frac{1}{2\pi} \log |z| + \frac{1}{2}(a+ib) \times \right. \\ \left. \times \sum_{r=0}^{\infty} \frac{\text{Exp}\{-(2\pi r + \beta)(a+ib) - i\lambda\}}{(2\pi r + \beta)(a+ib) + i\lambda} + \frac{1}{2}(a-ib) \sum_{r=1}^{\infty} \frac{\text{Exp}\{-(2\pi r - \beta)(a-ib) - i\lambda\}}{(2\pi r - \beta)(a-ib) + i\lambda} \right]. \quad (43)$$

(It should be noted in comparing this with equations A8 and A13 of Ref. 11 that the K function is not quite the same, in that the sign of its argument has been altered in order to make the notation more consistent. This means that the signs of z and z_1 must be changed in these equations of Ref. 11.)

In the numerical evaluation of the $J(z)$ function only the difficulty in connection with the infinite limit on the integral arises. This is dealt with in an exactly similar way to give

$$J(z) = U(z) + i\lambda e^{-i\lambda z} \left[\int_z^{-1} e^{i\lambda z_1} U(z_1) dz_1 - \frac{i}{2}(a+ib) \times \right. \\ \left. \times \sum_{r=0}^{\infty} \frac{\text{Exp}\{-(2\pi r + \beta)(a+ib) - i\lambda\}}{(2\pi r + \beta)(a+ib) + i\lambda} + \frac{i}{2}(a-ib) \sum_{r=1}^{\infty} \frac{\text{Exp}\{-(2\pi r - \beta)(a-ib) - i\lambda\}}{(2\pi r - \beta)(a-ib) + i\lambda} \right]. \quad (44)$$

The integrals occurring in equations (43) and (44) can be evaluated by numerical quadrature.

2.7. Calculation of Unsteady Vorticity.

In order to obtain the total unsteady induced velocities, it is necessary to add to equations (41) and (42) the velocities induced by movement of the steady vorticity given by equations (10) and (11). This gives

$$u = \int_0^1 J(\eta-x)\gamma(x) dx + \frac{q}{U} \int_0^1 M(\eta-x)\zeta(x) dx, \quad (45)$$

$$v = \int_0^1 K(\eta-x)\gamma(x) dx + \frac{q}{U} \int_0^1 N(\eta-x)\zeta(x) dx. \quad (46)$$

But on the blades the induced velocity v must match the blade velocity q . Hence, using equation (24),

$$\int_0^1 K(\eta-x)\gamma(x) dx = q + q\tau \int_0^1 N(\eta-x)\zeta_0(x) dx$$

for

$$0 < \eta < 1.$$

This is an integral equation for the unknown bound vorticity, γ . γ has two components, one independent of τ and one proportional to τ , and can therefore be written as

$$\gamma = q\gamma_q + q\tau\gamma_\tau, \quad (47)$$

where γ_q and γ_τ are solutions of the integral equations

$$\int_0^1 K(\eta-x)[\gamma_q, \gamma_\tau] dx = \left[1, \int_0^1 N(\eta-x)\zeta_0(x) dx \right] \quad (48)$$

for

$$0 < \eta < 1.$$

These equations have to be solved subject to the Joukowski condition at the trailing edge, which means that γ_q and γ_τ must be finite when $x = 1$.

Putting equations (24) and (47) into equation (45) gives for the induced velocity parallel to the blade chord

$$u = q \int_0^1 J(\eta-x)\gamma_q(x) dx + q\tau \int_0^1 J(\eta-x)\gamma_\tau(x) dx - q\tau \int_0^1 M(\eta-x)\zeta_0(x) dx. \quad (49)$$

It is convenient to write this as

$$u = qu_q + q\tau u_\tau, \quad (50)$$

where

$$u_q = \int_0^1 J(\eta-x)\gamma_q(x) dx, \quad (51)$$

and

$$u_\tau = \int_0^1 J(\eta-x)\gamma_\tau(x) dx - \int_0^1 M(\eta-x)\zeta_0(x) dx. \quad (52)$$

2.8. Calculation of Blade Force.

Equations (27) and (50) give the steady and unsteady components of the chordwise velocity induced at the reference blade by the vorticity on the other blades. At points just above and below the reference blade, denoted by suffices + and - respectively, the steady components are given by

$$u_{0+} = U + \tau U u_0 - \frac{1}{2}\zeta, \quad (53)$$

and

$$u_{0-} = U + \tau U u_0 + \frac{1}{2}\zeta. \quad (54)$$

Similarly the unsteady components are given by

$$u_+ = qu_q + q\tau u_\tau - \frac{1}{2}(\gamma + \epsilon), \quad (55)$$

and

$$u_- = qu_q + q\tau u_\tau + \frac{1}{2}(\gamma + \epsilon). \quad (56)$$

The complete velocities just above the reference blade are therefore given by

$$u = u_{0+} + u_+ e^{i\omega t}, \quad (57)$$

$$v = q e^{i\omega t}. \quad (58)$$

The pressure may now be calculated from the unsteady Bernoulli equation

$$\frac{\dot{p}}{\rho} + \frac{1}{2}u^2 + \frac{1}{2}v^2 + \frac{\partial\Phi}{\partial t} = F(t), \quad (59)$$

where Φ is the velocity potential and $F(t)$ is an arbitrary function of time only. Φ is given by

$$\partial\Phi/\partial x = u.$$

Therefore

$$\Phi = \int_0^x u dx_1.$$

Therefore

$$\partial\Phi/\partial t = \int_0^x (\partial u/\partial t) dx_1.$$

Using equation (57) for a point just above the reference blade

$$\frac{\partial\Phi_+}{\partial t} = i\omega e^{i\omega t} \int_0^x u_+ dx_1. \quad (60)$$

Putting equations (57), (58) and (60) in equation (59), and neglecting terms of second order in u and q , gives

$$-\frac{\dot{p}_+}{\rho} = \frac{1}{2}u_{0+}^2 + u_{0+}u_+ e^{i\omega t} + i\omega e^{i\omega t} \int_0^x u_+ dx - F(t).$$

There is an exactly similar equation for the pressure at a point just below the reference blade. Subtracting these gives the pressure difference across the blade, and the unsteady component of this is

$$-\frac{\dot{p}_- - \dot{p}_+}{\rho} = \left\{ u_{0-}u_- - u_{0+}u_+ + i\omega \int_0^x (u_- - u_+) dx_1 \right\} e^{i\omega t}.$$

Substituting from equations (53), (54), (55) and (56) gives

$$-\frac{\dot{p}_- - \dot{p}_+}{\rho} = \left\{ (U + \tau U u_0)(\gamma + \epsilon) + (qu_q + q\tau u_\tau)\zeta + i\omega \int_0^x (\gamma + \epsilon) dx_1 \right\} e^{i\omega t}.$$

This may be simplified using equation (32) to give

$$-\frac{\dot{p}_- - \dot{p}_+}{\rho} = \{ U\gamma + \tau U u_0(\gamma + \epsilon) + (u_q + \tau u_\tau)q\zeta \} e^{i\omega t}. \quad (61)$$

ϵ appears in this expression because it is not a true free vorticity. If true bound and free vorticities were used, only the true bound vorticity would appear in the expression for the pressure difference.

The fluctuating component of the upward force on the blade per unit length is then given by

$$F e^{i\omega t} = \int_0^c (\dot{p}_- - \dot{p}_+) dx.$$

Using equation (61) this gives

$$F = -\rho \int_0^1 \{U\gamma + \tau U u_0(\gamma + \epsilon) + (u_q + \tau u_\tau) q \zeta\} dx. \quad (62)$$

ζ has been expressed non-dimensionally by equation (24) and γ by equation (47). There is an exactly similar form for ϵ ,

$$\epsilon = q\epsilon_q + q\tau\epsilon_\tau, \quad (63)$$

where, from equation (31)

$$[\epsilon_q, \epsilon_\tau] = -i\lambda \int_0^{x_1} e^{i\lambda(x-x_1)} [\gamma_q, \gamma_\tau] dx. \quad (64)$$

Putting equations (24), (47) and (63) into equation (62) then gives

$$C_F = \frac{F}{\pi\rho U c q} = \frac{1}{\pi} \int_0^1 [-\gamma_q + \tau\{-\gamma_\tau - u_0(\gamma_q + \epsilon_q) + u_q \zeta_0\} + \tau^2\{-u_0(\gamma_\tau + \epsilon_\tau) + u_\tau \zeta_0\}] dx. \quad (65)$$

2.9. Matrix Form of the Equations.

The various integrals and integral equations which have been derived will have to be solved by numerical means. It is therefore convenient to put the equations into matrix form. First, a transformation to new independent variables, θ and ϕ , is made as in the usual thin-aerofoil theory for single aerofoils.

$$x = \frac{1}{2}(1 - \cos \theta),$$

$$\eta = \frac{1}{2}(1 - \cos \phi).$$

For example, equation (25), the integral equation for the steady vorticity, gives

$$\int_0^\pi \{V_0(\frac{1}{2} \cos \theta - \frac{1}{2} \cos \phi) - V_0(-\infty)\} \zeta_0 \frac{1}{2} \sin \theta d\theta = 1. \quad (66)$$

All the vorticities will be specified at $(n+1)$ points given by

$$\theta = \pi l/n$$

where l is an integer taking values from 0 to n . The values when $l = n$, at the trailing edge, will, however, be irrelevant since in equation (66) ζ_0 is multiplied by $\sin \theta$ which is zero. The same argument does not apply at the leading edge, since the vorticities become infinite there, although products such as $\zeta_0 \sin \theta$ remain finite.

The n values of ζ_0 can therefore be found to satisfy equation (64) at n points only, and these will be chosen to be given by

$$\phi = \pi(2m+1)/2n$$

where m is an integer taking values from 0 to $(n-1)$. These points have values of ϕ midway between the values of θ at which the vorticities have been specified.

It has previously been shown¹¹ that integrals of the type in equation (66) may be evaluated by the trapezoidal rule, except for a case when a logarithmic singularity occurs which requires special consideration. Then equation (66) may be written as a matrix equation,

$$A_0 Z = D, \quad (67)$$

where the matrices are defined in the table of matrices:

This gives the matrix of steady vorticity elements as

$$Z = A_0^{-1} D. \quad (68)$$

Similarly equation (28) gives

$$Y_0 = \tan \xi D - B_0 Z. \quad (69)$$

Equation (43) shows that the K function has a logarithmic singularity which means that equations (48) require special treatment. It is shown in Ref. 11 that these equations may be written

$$A \Gamma_q = D, \quad (70)$$

and

$$A \Gamma_r = QZ, \quad (71)$$

where A is the matrix given in the table of matrices.

Equation (51) gives

$$Y_q = B \Gamma_q. \quad (72)$$

Equation (52) gives

$$Y_r = B \Gamma_r - PZ. \quad (73)$$

Equation (64) is of a different type, since x_1 is the top limit of the integral. It has been shown by Watson¹² that this may be written

$$E_q = H \Gamma_q, \quad (74)$$

$$E_r = H \Gamma_r, \quad (75)$$

where H is the matrix given in the table.

Equation (65) gives

$$\pi C_F = -D^* \Gamma_q + \tau \{-D^* \Gamma_r - Y_0^* (\Gamma_q + E_q) + Y_q^* Z\} + \tau^2 \{-Y_0^* (\Gamma_r + E_r) + Y_r^* Z\} \quad (76)$$

where the notation * indicates a transposed matrix.

Eliminating the unknown matrices Z , Γ_q , Γ_r , E_q , E_r , Y_0 , Y_q and Y_r gives

$$\begin{aligned} \pi C_F = & -D^* A^{-1} D + \tau [D^* \{(A_0^*)^{-1} B_0^* - I \tan \xi\} \{H + I\} A^{-1} D + D^* \{(A^*)^{-1} B^* - A^{-1} Q\} A_0^{-1} D] + \\ & + \tau^2 [D^* \{(A_0^*)^{-1} B_0^* - I \tan \xi\} \{H + I\} A^{-1} Q A_0^{-1} D + D^* (A_0^*)^{-1} \{B A^{-1} Q - P\} A_0^{-1} D]. \end{aligned} \quad (77)$$

This is the required expression for the blade force. A special property which is of interest concerns the term $D^* (A_0^*)^{-1} P A_0^{-1} D$. The real part of the function $M(z)$ is an odd function of z . The real part of the matrix P is therefore an anti-symmetric matrix. Also the matrices A_0 and D are real so that $A_0^{-1} D$ is also real. Hence the real part of the term $D^* (A_0^*)^{-1} P A_0^{-1} D$ is equal to minus its transpose, and since it is just a single number it must be zero. It will be found that the flutter characteristics of a cascade are controlled only by the real part of C_F . Hence in calculations which are purely concerned with flutter the $D^* (A_0^*)^{-1} P A_0^{-1} D$ term can be omitted completely and the matrix P is not required.

3. Convergence.

This calculation has been programmed for EDSAC II, the electronic computer at the Cambridge University Mathematical Laboratory. With $n = 6$ the machine takes about 55 sec to calculate C_F for given values of s/c , ξ , β and λ and for a few values of α_1 .

The accuracy of the mathematical process can be assessed by doing calculations with increasing values of n and examining how the results tend to a limit. Some examples of this are given in Table 1. In most cases the convergence is very rapid, and $n = 6$ can be relied on for accurate results, but the convergence for cascades with small spacing and high stagger deteriorates. The results for the cascade with $s/c = 0.5$ and $\xi = 75^\circ$ show appreciable errors up to $n = 10$, which is the highest value of n which the present programme can handle.

4. Comparison with Previous Theoretical Results.

A comparison will now be made between the present theory and two other previous theories, those due to Sohngen³ and Shioiri⁶.

Sohngen's theory makes two assumptions additional to those made in the present theory. These are firstly that the spacing to chord ratio (s/c) of the blades is small and secondly that the phase angle (β) between adjacent blades is small. (The second assumption is not specifically stated by Sohngen, but is taken to be implied by the first assumption.) This enables a row of vortices to be replaced by a continuous vortex sheet, so that the vorticity on the blades is effectively spread out in the direction along the cascade. Transferred into the notation of the present report Sohngen's result is

$$C_F = \frac{s}{\pi c} \left[\left(B_{b0} - \frac{i}{\lambda} A_{b0} \right) + (2\tau \sec \xi) \left(B_{b1} - \frac{i}{\lambda} A_{b1} \right) + (2\tau \sec \xi)^2 \left(B_{b2} - \frac{i}{\lambda} A_{b2} \right) \right] \quad (78)$$

where

$$\begin{aligned} A_{b0} &= \frac{-1}{12N \cos \xi} \{ \lambda_n 12\sigma^2 \sin 2\xi + \\ &\quad + \lambda_n^2 [2\sigma^4 + 12\sigma^3 \cos \xi + 24\sigma^2 \cos^2 \xi + 24\sigma \cos 2\xi \cos \xi] - \\ &\quad - \lambda_n^4 (\sigma + 2 \cos \xi) [24 \cos \xi + 24\sigma \cos^2 \xi + 8\sigma^2 \cos \xi + \sigma^3] \}, \\ A_{b1} &= \frac{1}{2N} \{ \sigma^3 \sin \xi + \lambda_n \sigma^2 (\sigma \cos \xi - 2 \sin^2 \xi) + \\ &\quad + \lambda_n^3 (\sigma + 2 \cos \xi) (2\sigma \cos 2\xi + \sigma^2 \cos \xi) \}, \\ A_{b2} &= \frac{1}{4N} \{ \sigma^3 \sin^2 \xi + \lambda_n^2 \sigma (\sigma + 2 \cos \xi) (\sigma \sin^2 \xi - \cos \xi \cos 2\xi) \}, \\ B_{b0} &= \frac{-1}{4N \cos \xi} \{ 2\sigma^2 (\sigma + 2 \cos \xi)^2 - 8\sigma \sin \xi \cos \xi (\sigma + 2 \cos \xi) \lambda_n + \\ &\quad + \lambda_n^2 (\sigma^4 + 8\sigma^3 \cos \xi + 24\sigma^2 \cos^2 \xi + 32\sigma \cos^3 \xi + 16 \cos^2 \xi) \}, \\ B_{b1} &= \frac{-1}{2N} \left\{ \frac{1}{\lambda_n} \sigma^3 \cos \xi + (\sigma + 2 \cos \xi) \sigma^2 \sin \xi + \lambda_n \sigma \cos \xi (\sigma^2 + 4\sigma \cos \xi + 4 \cos 2\xi) \right\}, \\ B_{b2} &= -\frac{1}{4N} \sigma^2 \cos \xi, \end{aligned} \quad (79)$$

and

$$\left. \begin{aligned} \lambda_n &= -\frac{|\beta|}{\beta} \lambda, \\ \sigma &= |\beta| c/s, \\ N &= \sigma^2 + \lambda^2 (\sigma + 2 \cos \xi)^2. \end{aligned} \right\} \quad (80)$$

Sohnngen also gives expressions for the force in the chordwise direction and the moment about the leading edge both for this case of vibration perpendicular to the chord, and also for vibration parallel to the chord and for torsional vibration about the leading edge.

In Ref. 9 a theory was given in which the cascade is replaced by an actuator disc. The original analysis has been found to be incorrect and a corrected analysis is given in the Appendix to this report. The actuator-disc theory assumes that β and λ are both small. These assumptions can be fed into Sohnngen's analysis, by assuming that σ and λ (or λ_n) are both small and of the same order of magnitude in equations (79). It is then found that this result is identical with the corrected actuator-disc analysis. The actuator-disc analysis is therefore a special case of Sohnngen's theory. The actuator-disc analysis, however, remains of interest because it does not need to assume anything about the spacing or profile shape of the blades except that they must give constant air outlet angle and zero stagnation-pressure loss in quasi-steady flow.

Table 1 gives in the rows marked 'analytic' results from the actuator-disc theory for comparison with the results from the programme in four cases. At $s/c = 0.25$ the agreement is extremely close. At $s/c = 0.5$ the agreement is not quite so good. This is due to the fact that in the actuator-disc analysis and in Sohnngen's theory all deviation effects are neglected, whereas in the programme these effects are partially taken into account. At zero deflection the programme gives the correct answer, whereas the actuator-disc calculation shows a small error. At finite deflection both solutions will be slightly in error, but the programme should be more accurate.

Figs. 5 and 6 show some further comparisons with Sohnngen's theory. For small values of β there is seen to be close agreement, but as β increases the solutions diverge. This is the behaviour that would be expected from the assumption of small β in Sohnngen's theory.

The other theory with which comparison will be made is that due to Shioiri⁶. The most important assumption made in this theory, in addition to those made in the present report, is that in calculating the force on any blade, all the other blades are replaced by point vortices. There are also approximations in calculating the blade force, so that the expression for C_F is linear in τ , instead of being quadratic as in equation (77). This theory would therefore be expected to be best at high values of s/c . The comparison with Shioiri's calculations is shown in Figs. 7 and 8. Since Shioiri's assumptions are rather drastic, close agreement would not be expected, but the curves do show very similar trends.

These comparisons are also valuable in providing evidence that the programme is free from error, although it must be agreed that some of the terms in equation (77) do not receive a rigorous test in these comparisons. These checks are of course in addition to the usual checks on all the individual parts of the programme.

5. Flutter.

Up to this point it has been supposed that the blades are vibrating in a given manner and the aerodynamic forces on the blades have been calculated. This aerodynamic force must now be equated to the mechanical forces, in order that the conditions for self-excited vibration can be determined. It will be assumed that all the blades are identical and that there is no mechanical coupling through their roots. The motion of the blades which has been assumed in the calculations then corresponds to a normal mode of the system. Then the equation of motion for unit length of blade is

$$\mu \frac{d^2}{dt^2} (h_0 e^{i\omega t}) + \mu \omega_0 \frac{\delta}{\pi} \frac{d}{dt} (h_0 e^{i\omega t}) + \mu \omega_0^2 (h_0 e^{i\omega t}) = F e^{i\omega t},$$

where

μ = mass per unit length of blade,

ω_0 = natural frequency of blade in a vacuum,

and

δ = logarithmic decrement due to mechanical damping.

Writing the aerodynamic force F in terms of the force coefficient C_F and simplifying gives

$$\mu \left(-\omega^2 + i\omega_0\omega \frac{\delta}{\pi} + \omega_0^2 \right) = \pi\rho Uci\omega C_F.$$

For steady vibration both the real and imaginary parts of this equation must be satisfied. The real part gives

$$\left(\frac{\mu}{\pi\rho c^2} \right) \lambda \frac{\omega^2 - \omega_0^2}{\omega^2} = \mathcal{I}(C_F). \quad (81)$$

The imaginary part gives

$$\left(\frac{\mu}{\pi\rho c^2} \right) \lambda \frac{\omega_0}{\omega} \frac{\delta}{\pi} = \mathcal{R}(C_F). \quad (82)$$

Equation (81) determines the frequency at which flutter can occur. In practice the quantity $(\mu/\pi\rho c^2)$ is large, so that $(\omega_0^2 - \omega^2)$ is small and ω is very nearly equal to ω_0 .

Equation (82) relates the mechanical and aerodynamic damping, and is the condition for the vibration to be just self-excited. In all that follows the mechanical damping will be neglected, so that the condition for marginal flutter is

$$\mathcal{R}(C_F) = 0. \quad (83)$$

If the real part of C_F is positive there is a component of the aerodynamic force in phase with the blade velocity and the vibration will build up. Conversely if the real part of C_F is negative there is aerodynamic damping.

If a given cascade is considered with given values of β and λ , and α_1 (or τ) is regarded as a variable, then equations (77) and (83) give a quadratic equation for τ . This may have two roots giving two values of α_1 for which flutter is marginal. These values of α_1 are plotted against β for two cascades on Fig. 9. The marginal values of α_1 form loops, and inside these loops the real part of C_F is positive and flutter can occur.

Now if there is a large number of blades in the cascade, flutter can occur at any value of the phase angle β . Taking as an example the cascade with $\xi = 15^\circ$ on Fig. 9 this means that flutter will occur at any value of α_1 between points A and B, and also between points C and D. These are the critical values of α_1 and the programme has been arranged to find them. It operates by hunting for maxima and minima in the graphs of τ against β . It will be seen that there are also non-significant maxima and minima at points E and F which may be found by the programme. These non-significant roots disappear at higher values of λ and ξ . The zero stagger ($\xi = 0$) case is peculiar since there are only two significant roots at A' and C' (Fig. 9) with two non-significant roots at E' and G'.

The results for the critical values of α_1 are shown in Figs. 10 to 13. These figures show frequency parameter, λ , plotted against deflection, which is here taken as $\alpha_1 - \xi$, deviation being neglected. The results are shown for compressor and turbine cascades separately, and for space/chord ratios of 1.0 and 0.5. Flutter is predicted if the operating point is below the line drawn, that is if the frequency parameter is less than a critical value or if the flow velocity is greater than a critical value. The curves for compressor cascades (Figs. 12 and 13) are seen to turn downwards for high

deflections. The curves for turbine cascades also turn downwards but only at very high deflections which are of no practical interest and therefore not shown on Figs. 10 and 11. ($\xi = 0$ is an exception to this statement.)

The corresponding critical phase angles are shown in Figs. 14 and 15. A further interesting result is that if $\beta = 0$ then no flutter can be found, so that the flutter would be stopped by connecting the tips of blades together thus making them all move in phase.

Sohnngen⁸ has shown that for zero stagger cascades his theory gives a very simple result. This is that the critical value of λ is given by

$$\lambda = \frac{1}{4} \tan \alpha_1, \quad (84)$$

and the corresponding phase angle is given by

$$\sigma = |\beta|c/s = 2. \quad (85)$$

Equation (84) is compared with the results from the programme on Fig. 16, and it is seen that agreement with the $s/c = 0.5$ calculation is very good. The critical phase angles (very nearly independent of λ from the programme) are as follows:

s/c	$\beta/2\pi$ (Sohnngen)	$\beta/2\pi$ (Programme)
1.0	0.318	0.173
0.5	0.159	0.123

6. Comparison with Experimental Results.

In this section the present theory will be compared with the results of two experimental investigations by Shioiri⁷ and Leclerc⁸.

Shioiri's experiment was done in a cascade with seven blades free to vibrate, the first and last of these blades being mechanically coupled so as to simulate an infinite cascade. Flutter was observed with $\beta/2\pi = 1/6$ for the compressor cascades and with $\beta/2\pi = 5/6$ for the turbine cascades. These values of β have therefore been used in the theoretical calculations. The comparisons are shown in Figs. 17 and 18. The agreement between theory and experiment for the turbine cascades is quite good, but for the compressor cascades the theoretical flutter velocity considerably exceeds the experimental flutter velocity. On the whole the general tendencies of the theory are confirmed by the experiment. Shioiri shows somewhat better agreement between his own theory and his experiments. It is possible that, in neglecting some of the terms arising from the steady vorticity distribution on the blades, Shioiri's theory makes some allowance for the camber of the aerofoils.

The other set of experiments with which comparison will be made is that due to Leclerc⁸. The damping in a cascade of zero cambered blades was measured and was found to go to zero for two arrangements of turbine cascades. The results are as follows:

s/c	0.587	
ξ	45°	
Incidence	16.7°	17.7°
Critical λ by expt.	0.091	0.094
Critical λ by theory	0.080	0.085

The agreement is good.

7. Conclusions.

The main conclusion of this report is that unstalled bending flutter of compressor and turbine blades is predicted if the gas flow velocity exceeds a certain critical value. Current gas turbines are usually fairly close to this limit, but axial compressors are usually well clear of the critical velocity, and stalled flutter is likely to be a much more serious limitation. The blading at the low-pressure end of steam turbines usually works in a flow velocity well in excess of the critical value calculated here, and this could explain the need for lacing wires in these turbines. Any such device which makes all the blades more in phase stops this type of flutter.

The theory presented here shows substantial agreement with previous theories due to Sohngen³ and Shioiri⁶, particularly in those regions where good agreement would be expected. It is believed, however, that the present theory is much more accurate than any of the previous theories, although there are still idealizations of a number of effects which are likely to have considerable influence in actual machines. The most important of these effects neglected in the theory appear to be:

- (a) Mechanical damping.
- (b) Mistuning of the blades in any row.
- (c) Effect of blade camber.
- (d) Compressibility.
- (e) Three-dimensional flow effects.
- (f) Torsional motion in the fundamental bending mode.

The effects (a) and (b) in this list will always have the result of raising the flutter velocity and are therefore favourable. The remaining effects may be favourable or unfavourable.

In spite of these approximations, it is suggested that Figs. 10, 11, 12 and 13 be used as a design rule for turbo-machine blading, the flow angles being taken at the tips of the blades. It will probably be necessary to use an empirical factor on the critical flow velocity in order to allow for the various unknowns, and such a factor can only be determined on the basis of practical experience. If in any design the critical flow velocity was found to be exceeded, then it would be necessary to increase the chord of the blades, fit lacing wires, or connect the tips of the blades together through shrouds.

Further theoretical work to clear up the effect of at least some of the unknowns is desirable. In particular it should not be too difficult to modify the present programme to allow for the effects of blade camber and the presence of some torsional motion in the fundamental bending mode of the blade. Shioiri⁷ has included this latter effect in his work and has shown that it is important.

NOTATION

Some of the notation and axes used are shown on Fig. 2.

$F e^{i\omega t}$	Unsteady aerodynamic force on blade
$J(z), K(z)$	Functions giving induced velocities, including wake effects
$M(z), N(z)$	Functions for velocities induced by displacement of steady vorticity
N	See equation (80)
$U(z), V(z)$	Functions for velocities induced by unsteady vorticity
U	Mainstream velocity
$U_0(z), V_0(z)$	Functions $U(z)$ and $V(z)$ when $\beta = 0$
a	$= (c/s) \cos \xi$
b	$= (c/s) \sin \xi$
c	Chord (this is put equal to unity)
f	Function given by equation (7)
g	Function given by equation (14)
h_m	Displacement of m th blade
i	$= \sqrt{-1}$. Indicates component leading 90° in phase
l, m	Integers
n	Order of approximation
p	Static pressure
$q e^{i\omega t}$	Translational velocity of blade due to its vibration
r	Integer
s	Cascade spacing
t	Time
u, v	Induced velocities
u_0	Steady component of u {see equation (27)}
u_q	Unsteady component of u independent of τ {see equation (50)}
u_τ	Unsteady component of u proportional to τ {see equation (50)}
x, y	Rectangular co-ordinates
z	$= (\eta - x)$
α_1	Air inlet angle
α_2	Air outlet angle

NOTATION—*continued*

β	Phase angle between adjacent blades
$\gamma e^{i\omega t}$	Bound vorticity
γ_a	Component of γ independent of τ
γ_τ	Component of γ proportional to τ
δ	Logarithmic decrement due to mechanical damping
$\epsilon e^{i\omega t}$	Pseudo free vorticity
ϵ_a	Component of ϵ independent of τ
ϵ_τ	Component of ϵ proportional to τ
ζ	Steady vorticity
$\zeta_0 = -\zeta/\tau U$	
η	Co-ordinate for induced velocity
θ	Variable defined by $x = \frac{1}{2}(1 - \cos \theta)$
$\lambda = \omega c/U$	frequency parameter
μ	Mass per unit length of blade
ξ	Stagger angle
ρ	Gas density
σ	See equation (80)
τ	Variable used to specify incidence of steady flow
τ_2	Variable used to specify deviation
ϕ	Variable defined by $\eta = \frac{1}{2}(1 - \cos \phi)$
χ	Variable defined by equation (5)
ω	Angular frequency of vibration
Γ_m	Strength of m th vortex in row
Φ	Velocity potential

Suffices + and – refer to points just above and below the surface of the blade respectively.

Σ Indicates summation

$\sum'_{r=1}^n$ Indicates summation in which the n th term is halved.

Table of Matrices

In all cases the element given is in the l th column and m th row ($0 \leq l \leq n-1$, $0 \leq m \leq n-1$).
Also

$$z = \frac{1}{2} \left\{ \cos \frac{\pi l}{n} - \cos \frac{\pi(2m+1)}{2n} \right\}$$

Matrix	Order	Element
Z	$n \times 1$	$\left. \begin{aligned} &(\pi/2n)\zeta_0(\pi m/n) \sin(\pi m/n) \\ &(\pi/2n)\gamma_q(\pi m/n) \sin(\pi m/n) \\ &(\pi/2n)\gamma_r(\pi m/n) \sin(\pi m/n) \\ &(\pi/2n)\epsilon_q(\pi m/n) \sin(\pi m/n) \\ &(\pi/2n)\epsilon_r(\pi m/n) \sin(\pi m/n) \end{aligned} \right\} \text{First element halved}$
Γ_q	$n \times 1$	
Γ_r	$n \times 1$	
E_q	$n \times 1$	
E_r	$n \times 1$	
D	$n \times 1$	1
I	$n \times n$	Unit matrix
A_0	$n \times n$	$V_0(z) - V_0(-\infty)$
B_0	$n \times n$	$U_0 \left(\frac{1}{2} \cos \frac{\pi l}{n} - \frac{1}{2} \cos \frac{\pi m}{n} \right) - U_0(-\infty)$
A	$n \times n$	$K(z) + i\lambda e^{-i\lambda z} \left[\frac{1}{\pi} \log_e 2 + \frac{1}{\pi} \sum_{r=1}^n \frac{1}{r} \cos \frac{\pi r(2m+1)}{2n} \cos \frac{\pi r l}{n} - \frac{1}{2\pi} \log z \right]$
B	$n \times n$	$J \left(\frac{1}{2} \cos \frac{\pi l}{n} - \frac{1}{2} \cos \frac{\pi m}{n} \right)$
Y_0	$n \times 1$	$u_0(\pi m/n)$
Y_q	$n \times 1$	$u_q(\pi m/n)$
Y_r	$n \times 1$	$u_r(\pi m/n)$
H	$n \times n$	$-\frac{i\lambda}{2n} \left[\frac{\pi m}{n} + 2 \sum_{r=1}^{n-1} \frac{1}{r} \sin \frac{\pi r m}{n} \cos \frac{\pi r l}{n} \right] \times$ $\times \left[\text{Exp} \left\{ \frac{\lambda}{2} \left(\cos \frac{\pi m}{n} - \cos \frac{\pi l}{n} \right) \right\} \right] \sin \pi m/n$
P	$n \times n$	$M \left(\frac{1}{2} \cos \frac{\pi l}{n} - \frac{1}{2} \cos \frac{\pi m}{n} \right)$
Q	$n \times n$	$N(z)$

REFERENCES

- | <i>No.</i> | <i>Author(s)</i> | <i>Title, etc.</i> |
|------------|--------------------------------|--|
| 1 | J. F. Shannon | Vibration problems in gas turbines, centrifugal and axial compressors. A.R.C. R. & M. 2226. March, 1945. |
| 2 | C. Bellenot and J. L. d'Épinay | Self-induced vibrations of turbomachine blades.
<i>Brown Boveri Review</i> , Vol. 37, p. 368. 1950. |
| 3 | H. Sohngen | Luftkrafte an einem schwingenden schaufelkranz kleiner teilung.
<i>Z.A.M.P.</i> , Vol. 4, p. 267. 1953. |
| 4 | D. S. Whitehead | The aerodynamics of axial compressor and turbine blade vibration. Cambridge University Ph.D. Thesis. 1957. |
| 5 | R. Skarecky | Samobuzene kmitani lopatek v lopatkovych mrizich.
<i>Proudeni v Lopatkovych Strojich</i> , p. 259. 1958. |
| 6 | J. Shioiri | Non-stall normal mode flutter in annular cascade. Part I. Theoretical study.
<i>Trans. Jap. Soc. Aero. Eng.</i> , Vol. 1, p. 26. 1958. |
| 7 | J. Shioiri | Non-stall normal mode flutter in annular cascade. Part II. Experimental study.
<i>Trans. Jap. Soc. Aero. Eng.</i> , Vol. 1, p. 36. 1958. |
| 8 | J. Leclerc | Amortissement aerodynamique des vibrations de flexion dans une grille a basse vitesse.
<i>La Recherche Aeronautique</i> , No. 71, p. 59. 1959. |
| 9 | D. S. Whitehead | The vibration of cascade blades treated by actuator disc methods.
<i>Proc. I. Mech. E.</i> , Vol. 173, p. 555. 1959. |
| 10 | W. G. Molyneux | An approximate theoretical approach for the determination of oscillatory aerodynamic coefficients for a helicopter rotor in forward flight.
<i>Aero. Quart.</i> , Vol. XIII, pp. 235-254. August, 1962. |
| 11 | D. S. Whitehead | Force and moment coefficients for vibrating aerofoils in cascade. A.R.C. R. & M. 3254. February, 1960. |
| 12 | E. J. Watson | Formulae for the computation of the functions employed for calculating the velocity distribution about a given aerofoil. A.R.C. R. & M. 2176. May, 1945. |

APPENDIX

Correction to Actuator-Disc Analysis

Introduction.

In a previous paper⁹ a theory was given which should give the forces on vibrating blades with finite deflection if the frequency parameter and the phase angle between adjacent blades are both small. This theory was found to be in disagreement with the theory given in the present paper, and further investigation has shown that the actuator-disc theory requires correction in this case.

In the actuator-disc theory the flow fields upstream and downstream of the cascade are considered, and the scale of these effects is very much larger than the chord or spacing of the blades. On this scale the cascade is therefore replaced by an actuator disc. These two flow fields are then matched across the actuator disc, which behaves like the cascade with steady flow through it.

It is the set of equations relating to the cascade which has been found to require correction.

The notation used in this Appendix is the same as in the original paper and is not quite the same as in the main body of the present report. In particular the axes are chosen normal to and along the cascade direction, instead of being aligned with the blade chords. The notation is illustrated in Fig. 19.

Cascade Considerations.

Fig. 19 shows the cascade of blades POQ in their equilibrium position, and also in a position P'O'Q' where they have been displaced due to the vibration. There are $N/2$ blades between P and O, and $N/2$ blades between O and Q. N is large enough so that local effects of individual blades are negligible, but the phase angle is small enough so that the phase angle between the vibration of the blade at P and the vibration of the blade at Q is small. The displacements of the blades at O, P and Q are respectively,

$$h_0 e^{i\omega t}, \quad h_0 e^{i(\omega t + N\beta/2)}, \quad h_0 e^{i(\omega t - N\beta/2)}.$$

The direction of the displacements is specified by the angle θ . Then the small angle ϕ between the line P'Q' and PQ is given by

$$\tan \phi = \frac{h_0 e^{i(\omega t + N\beta/2)} \sin \theta - h_0 e^{i(\omega t - N\beta/2)} \sin \theta}{Ns + h_0 e^{i(\omega t + N\beta/2)} \cos \theta - h_0 e^{i(\omega t - N\beta/2)} \cos \theta}.$$

Since h_0 is small compared with s and the phase angle $N\beta$ is also small this gives to first order,

$$\phi = ih_0 \beta \sin \theta e^{i\omega t} / s.$$

ϕ is the angle through which the cascade has turned due to its vibration.

Since

$$qe^{i\omega t} = i\omega h_0 e^{i\omega t},$$

then

$$\phi = q\beta \sin \theta e^{i\omega t} / \omega s. \tag{A1}$$

ϕ is of the same order of magnitude as q , since β and ω are both small but of the same order of magnitude.

The velocity of the air upstream of the blades relative to the blades is given by

$$u_{r1} = U + (u_{01} + q \sin \theta) e^{i\omega t}, \tag{A2}$$

$$v_{r1} = V_1 + (v_{01} - q \cos \theta) e^{i\omega t}, \tag{A3}$$

and similarly downstream the relative velocities are

$$u_{r2} = U + (u_{02} + q \sin \theta) e^{i\omega t}, \quad (\text{A4})$$

$$v_{r2} = V_2 + (v_{02} - q \cos \theta) e^{i\omega t}. \quad (\text{A5})$$

By continuity, the relative velocity normal to the cascade is conserved. Hence

$$u_{r1} \cos \phi + v_{r1} \sin \phi = u_{r2} \cos \phi + v_{r2} \sin \phi.$$

Substituting from equations (A1) to (A5) gives for the first-order terms

$$(u_{01} - u_{02}) + (V_1 - V_2) \sin \theta q \beta / \omega s = 0. \quad (\text{A6})$$

This may be compared with equation (10) of Ref. 9, which gave simply $u_{01} = u_{02}$. The extra term is due to the inclination, ϕ , of the cascade, which was previously neglected.

Although the blades are displaced due to the vibration they do not twist. Since deviation effects are being neglected, the relative air outlet angle is constant and is assumed to be the same as the angle at which the blades vibrate, θ . This gives

$$v_{r2}/u_{r2} = \tan \theta.$$

Substituting from equations (A4) and (A5), and noting that for the steady flow $V_2 = U \tan \theta$, gives

$$(v_{02} - q \cos \theta) = (u_{02} + q \sin \theta) \tan \theta. \quad (\text{A7})$$

This equation is unmodified.

The equation giving the vorticity, ζ_{02} , also does not require any modification. Putting the stagnation pressure loss terms in equation (14) of Ref. 9 equal to zero, putting ζ_{01} (the upstream vorticity) equal to zero and evaluating some simple derivatives gives

$$\frac{U \zeta_{02}}{\omega} = i(v_{01} - v_{02}) + (V_1 - V_2) \cos \theta \frac{i\beta q}{\omega s}. \quad (\text{A8})$$

This equation can also be derived by considering the circulation round a control surface which encloses the blades between P and Q (Fig. 19). The rate of change of this circulation must equal the rate at which vorticity leaves the control surface. In evaluating this last rate it is necessary to include the rate at which bound vorticity is carried into or out of the control surface by movement of the blades.

It is now necessary to calculate the force acting on each blade, and it will be convenient to start from axes perpendicular and parallel to the displaced cascade. These axes are turned through an angle ϕ from the original axes. The air velocities relative to the blades in these directions are

$$u_{r1}' = u_{r1} \cos \phi + v_{r1} \sin \phi = u_{r2}', \quad (\text{A9})$$

$$v_{r1}' = -u_{r1} \sin \phi + v_{r1} \cos \phi, \quad (\text{A10})$$

$$v_{r2}' = -u_{r2} \sin \phi + v_{r2} \cos \phi. \quad (\text{A11})$$

Let the forces exerted by the air on each blade per unit length be X' and Y' in these directions. These are the average forces for the N blades between P' and Q'. Then

$$NX' = (\hat{p}_1 - \hat{p}_2) P' Q'.$$

Since the flow is quasi-steady with no losses the pressure difference across the cascade is given by

$$\frac{p_1}{\rho} + \frac{1}{2}u_{r1}'^2 + \frac{1}{2}v_{r1}'^2 = \frac{p_2}{\rho} + \frac{1}{2}u_{r2}'^2 + \frac{1}{2}v_{r2}'^2,$$

giving

$$(p_1 - p_2) = \frac{1}{2}\rho(v_{r2}'^2 - v_{r1}'^2).$$

Also the length P'Q' is given by

$$\begin{aligned} P'Q' &= Ns + h_0 e^{i(\omega t + N\beta/2)} \cos \theta - h_0 e^{i(\omega t - N\beta/2)} \cos \theta, \\ &= Ns + ih_0 N\beta \cos \theta e^{i\omega t}. \end{aligned}$$

This gives

$$X' = \frac{1}{2}\rho(v_{r2}'^2 - v_{r1}'^2)(s + ih_0\beta \cos \theta). \quad (\text{A12})$$

The force Y' is given by

$$NY' = \rho u_{r1}'(v_{r1}' - v_{r2}')P'Q'.$$

This gives

$$Y' = \rho u_{r1}'(v_{r1}' - v_{r2}')(s + ih_0\beta \cos \theta). \quad (\text{A13})$$

The force in the direction of the vibration is then

$$-X' \sin(\theta - \phi) + Y' \cos(\theta - \phi).$$

The first-order component of this is $F e^{i\omega t}$. Using equations (A1) to (A6) and (A9) to (A13) it is found after some reduction that F is given by

$$\begin{aligned} \frac{F}{\rho s} &= (V_1 v_{01} - V_2 v_{02}) \sin \theta + (V_1 u_{02} - V_2 u_{01}) \cos \theta + \\ &+ U(v_{01} - v_{02}) \cos \theta - U(u_{01} - u_{02}) \cos^2 \theta \operatorname{cosec} \theta. \end{aligned} \quad (\text{A14})$$

(A6), (A7), (A8) and (A14) are the equations required. It may be seen that for the zero-mean-deflection case when $V_1 = V_2$ they give the same results as the corresponding equations in the original paper. It is therefore only the finite deflection case which requires correction.

Actuator-Disc Considerations.

These considerations do not require modification. Equations (3) and (4) of the original report⁹ with the upstream vorticity put equal to zero give

$$u_{02} + iv_{02} = \frac{U\zeta_{02}/\omega}{-1 + (V_2/V_s) + i(U/V_s)}, \quad (\text{A15})$$

and

$$u_{01} + iv_{01} = 0, \quad (\text{A16})$$

where V_s is the speed of propagation of the disturbance along the cascade and is assumed to be positive. V_s is related to β as follows,

$$\frac{V_s}{U} = -\frac{\omega s}{U\beta}. \quad (\text{A17})$$

The results that follow therefore only hold when β is negative.

Elimination.

Using equations (A6), (A7), (A8), (A14), (A15) and (A16) the unknowns u_{01} , v_{01} , u_{02} , v_{02} and ζ_{02} may be eliminated. The result is

$$\begin{aligned}
 C_F &= \frac{F}{\pi \rho c q U \sec \theta} \\
 &= \frac{s}{\pi c} \sec \theta [\tau^2 \{-x^2(1+t^2)^2\} - \\
 &\quad - i\tau^2 \{x^3 t^3(1+t^2)^2 - 2x(1-t^2)\} + \\
 &\quad + \tau \{-x^3(1+t^2)^2 - 2x^2 t(1+t^2) - 4x(1-t^2)\} - \\
 &\quad - i\tau \{x^3 t(1+t^2)^2 - 2x^2 t^2(1+t^2)\} + \\
 &\quad + \{-2x^2(1+t^2) + 4xt - 4\} - \\
 &\quad - i\{-2x^2 t(1+t^2) - 2x(1-t^2)\} \{4 + x^2(1+t^2)^2\}^{-1}, \tag{A18}
 \end{aligned}$$

where

$$x = U/V_s = -U\beta/\omega s = -\beta c \cos \theta/s\lambda,$$

$$t = \tan \theta,$$

$$\tau = (\tan \alpha_1 - \tan \theta) \cos^2 \theta.$$

If β is positive, then the cascade must be drawn upside down. This changes the sign of V_s , θ , x , t and τ . It will be seen that the same effect can be obtained in equation (A18) by changing the sign of i , so that C_F is replaced by its complex conjugate.

It appears from equation (A18) that it is always possible to find values of x which make the real part of C_F positive for any value of τ (except zero). The corrected actuator-disc theory therefore predicts that when the frequency parameter is small bending flutter will always occur unless the deflection is zero.

TABLE 1

Tests on Convergence and Comparison with Actuator Disc Theory

s/c	ξ	$\beta/2\pi$	λ	n	$\mathcal{R}(C_F)$	$\mathcal{I}(C_F)$	$\mathcal{R}(C_F)$	$\mathcal{I}(C_F)$	$\mathcal{R}(C_F)$	$\mathcal{I}(C_F)$
					$\alpha_1 = 0$		$\alpha_1 = 45^\circ$		$\alpha_1 = -45^\circ$	
0.25	0	$1 \cdot 10^{-5}$	$2 \cdot 10^{-5}$	6	-0.15722	0.01235	0.76507	0.02479	-1.23472	0.02474
				7	-0.15722	0.01235	0.76507	0.02479	-1.23472	0.02475
				Analytic	-0.15719	0.01235	0.76520	0.02470	-1.23480	0.02470
0.5	0	$1 \cdot 10^{-5}$	$1 \cdot 10^{-5}$	4	-0.31338	0.02453	1.48575	0.07568	-2.41395	0.06832
				6	-0.31338	0.02453	1.48574	0.07568	-2.41395	0.06832
				Analytic	-0.31438	0.02470	1.53040	0.04940	-2.46960	0.04940
0.25	30	$1 \cdot 10^{-5}$	$2 \cdot 10^{-5}$	5	-0.56117	0.13281	0.13341	-0.29801	-1.35721	0.20265
				6	-0.56117	0.13282	0.13341	-0.29801	-1.35721	0.20266
				Analytic	-0.56115	0.13281	0.13347	-0.29802	-1.35721	0.20262
0.5	30	$1 \cdot 10^{-5}$	$1 \cdot 10^{-5}$	5	-1.10774	0.27467	0.25368	-0.59796	-2.68789	0.44252
				6	-1.10770	0.27472	0.25362	-0.59799	-2.68785	0.44270
				Analytic	-1.12230	0.26562	0.26693	-0.59604	-2.71442	0.40524
0.5	0	0.123	0.500	6	-0.57779	0.09130	-0.25000	0.31957	-1.00089	0.10654
				7	-0.57780	0.09130	-0.24999	0.31959	-1.00090	0.10654

TABLE 1—*continued*

s/c	ξ	$\beta/2\pi$	λ	n	$\mathcal{R}(C_F)$	$\mathcal{I}(C_F)$	$\mathcal{R}(C_F)$	$\mathcal{I}(C_F)$
					$\alpha_1 = 60^\circ$		$\alpha_1 = -57.640^\circ$	
0.5	60	0.889	0.500	6	-0.40087	0.18581	0.00000	-0.31102
				7	-0.40085	0.18524	0.00126	-0.29816
				8	-0.40068	0.18520	0.00100	-0.30412
				9	-0.40070	0.18526	0.00122	-0.30078
				10	-0.40072	0.18525	0.00101	-0.30243
					$\alpha_1 = 60^\circ$		$\alpha_1 = -54.412^\circ$	
1.0	60	0.779	0.500	6	-0.51265	0.28602	0.00001	-0.23575
				7	-0.51265	0.28602	-0.00024	-0.23582
					$\alpha_1 = 75^\circ$		$\alpha_1 = 0$	
0.5	75	0.940	0.200	6	-0.23898	0.23587	0.00140	0.04741
				7	-0.23613	0.23178	-0.01061	-0.07881
				8	-0.23247	0.23626	-0.00371	0.08233
				9	-0.23462	0.23530	-0.00908	0.01364
				10	-0.23466	0.23446	-0.00493	0.01282
					$\alpha_1 = 75^\circ$		$\alpha_1 = 0$	
1.0	75	0.800	0.200	6	-0.26926	0.42595	0.05770	0.22070
				7	-0.26925	0.42595	0.05761	0.22212
				8	-0.26925	0.42595	0.05754	0.22218
				9	-0.26925	0.42595	0.05749	0.22208
				10	-0.26925	0.42595	0.05746	0.22208

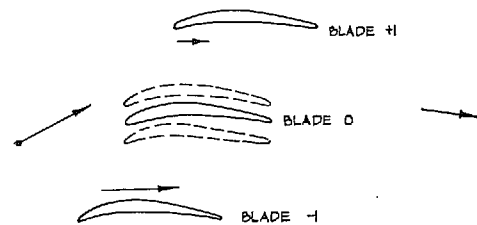


FIG. 1. Physical explanation of effect.

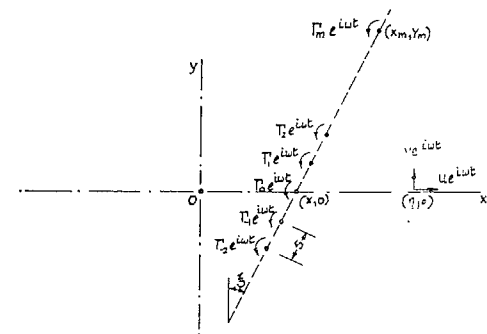


FIG. 3. Row of unsteady vortices.

30

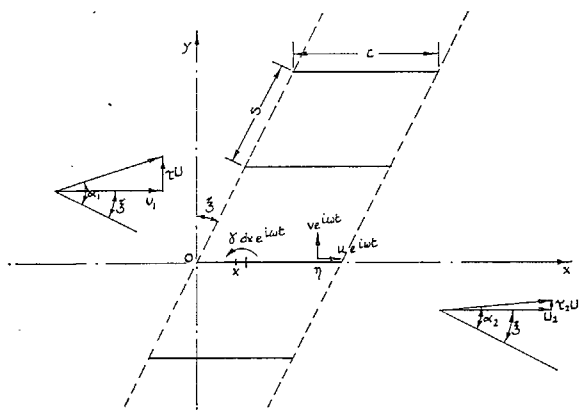


FIG. 2. Notation.

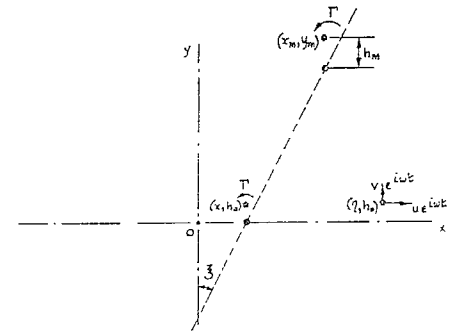


FIG. 4. Row of displaced steady vortices.

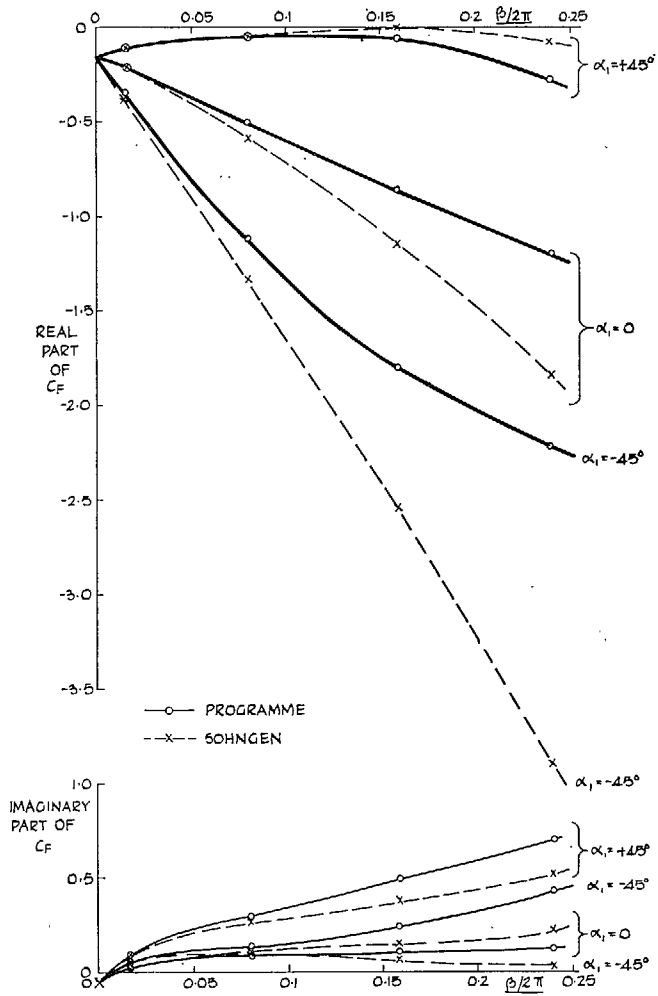


FIG. 5. Comparison with Sohngen's theory:
 $s/c = 0.5$, $\xi = 0$, $\lambda = 0.25$.

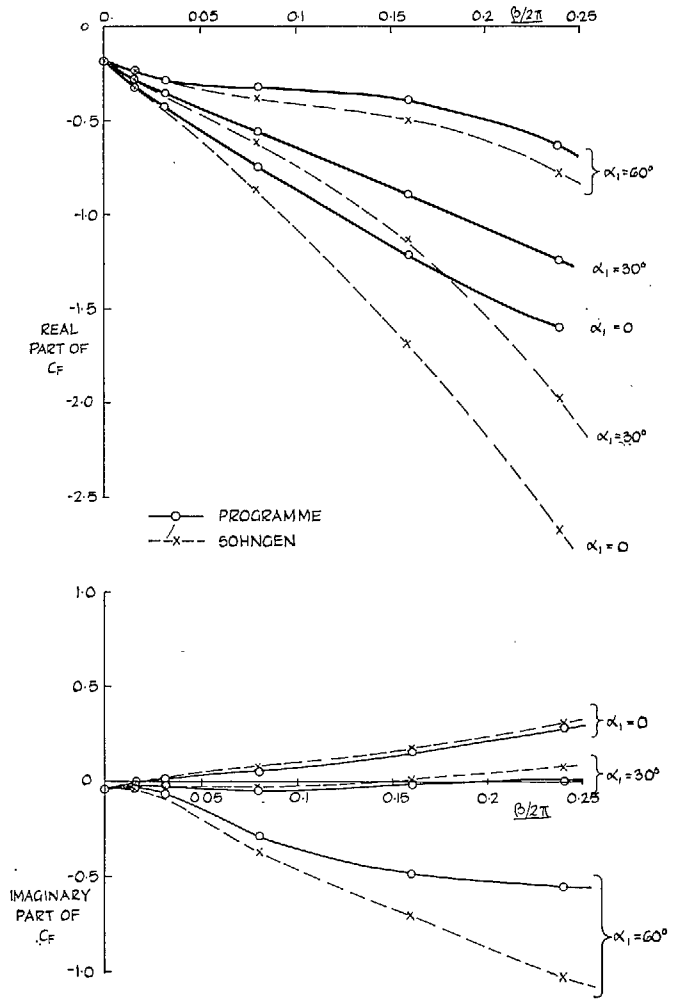


FIG. 6. Comparison with Sohngen's theory:
 $s/c = 0.5$, $\xi = 30^\circ$, $\lambda = 0.25$.

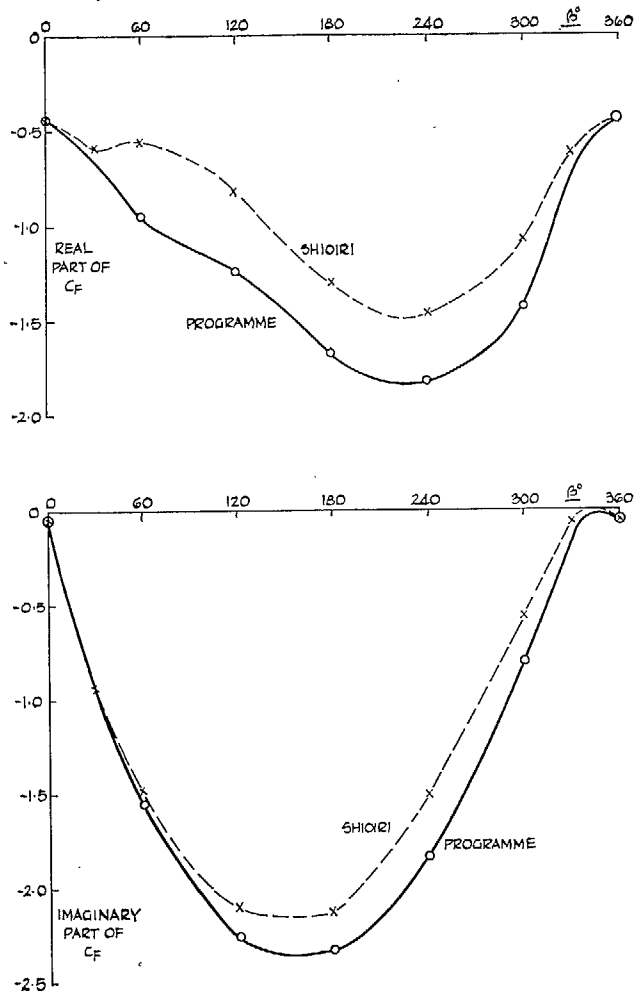


FIG. 7. Comparison with Shioiri's theory:
 $s/c = 1$, $\xi = 45^\circ$, $\lambda = 0.2$, $\alpha_1 = 65.48^\circ$.

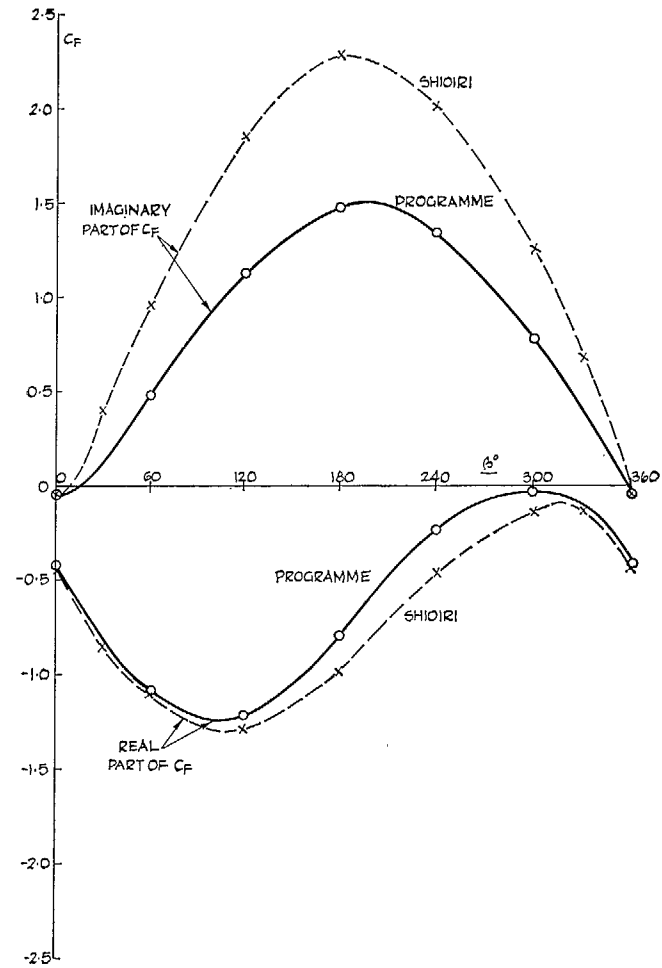


FIG. 8. Comparison with Shioiri's theory:
 $s/c = 1$, $\xi = 45^\circ$, $\lambda = 0.2$, $\alpha_1 = -10.85^\circ$.

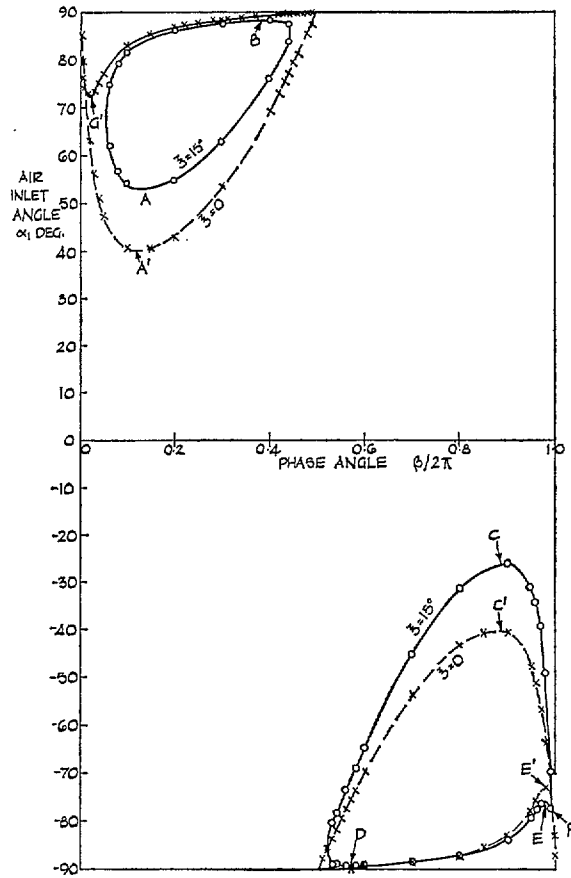


FIG. 9. Flutter margins: $s/c = 0.5$, $\lambda = 0.2$.

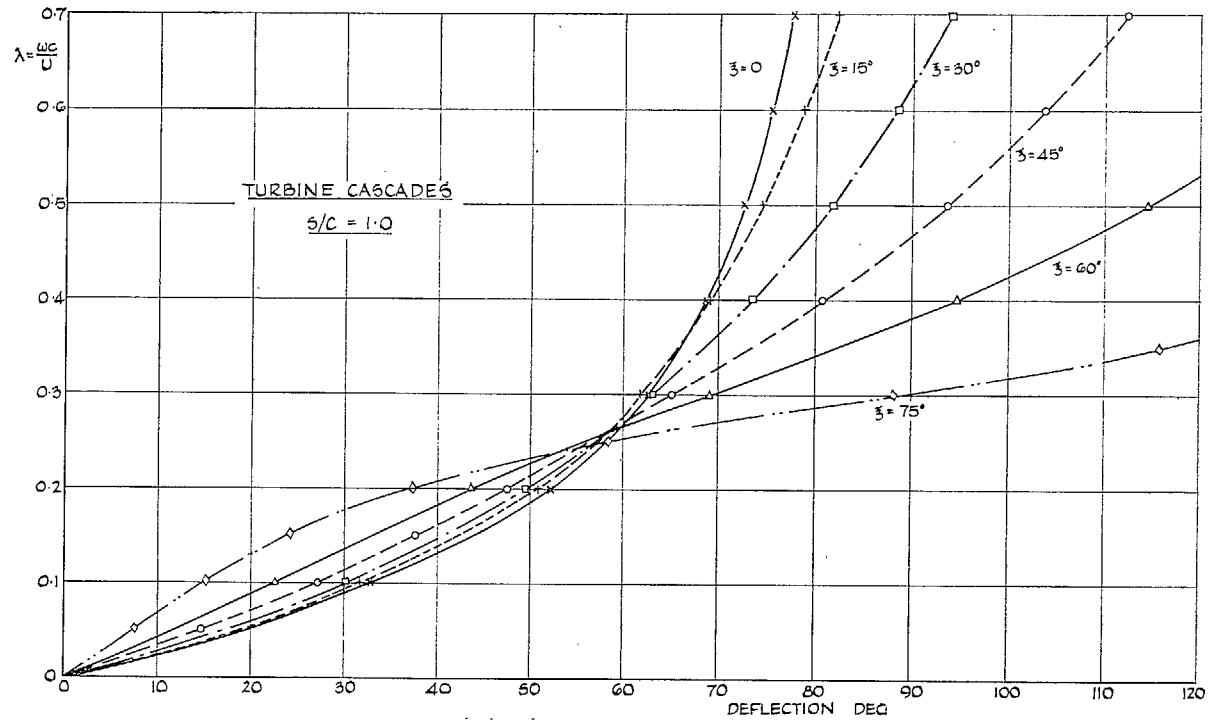


FIG. 10. Critical frequency parameter for flutter.

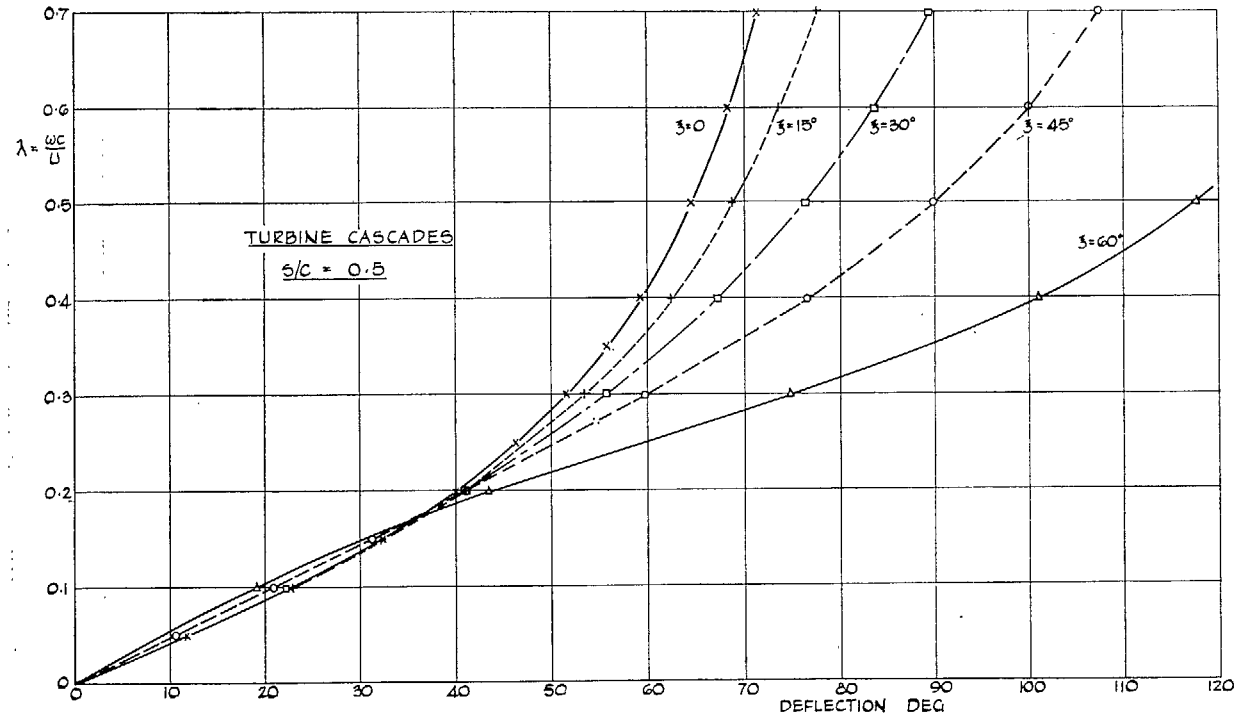


FIG. 11. Critical frequency parameter for flutter.

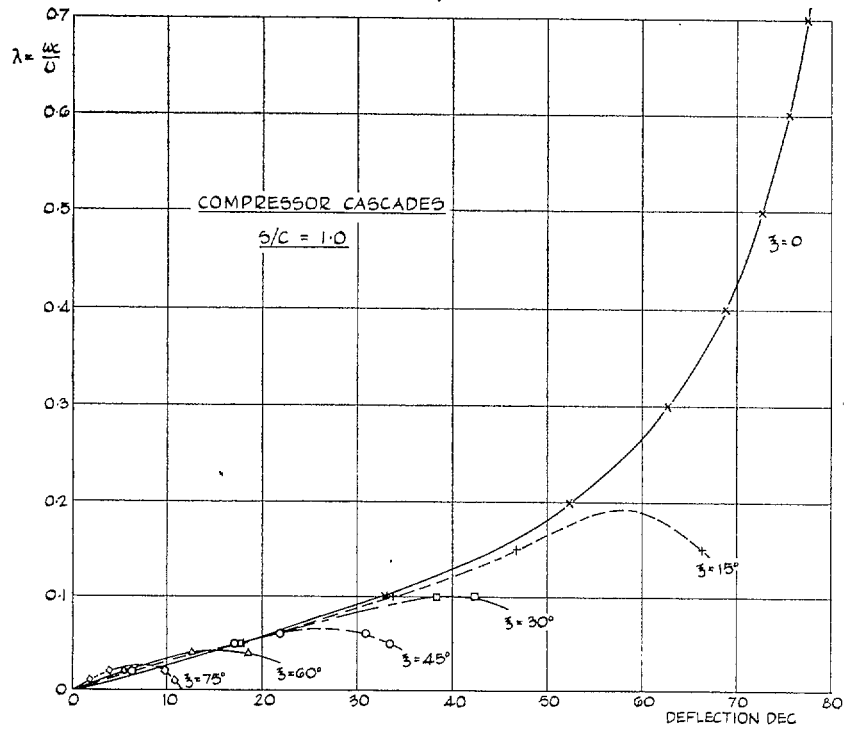


FIG. 12. Critical frequency parameter for flutter.

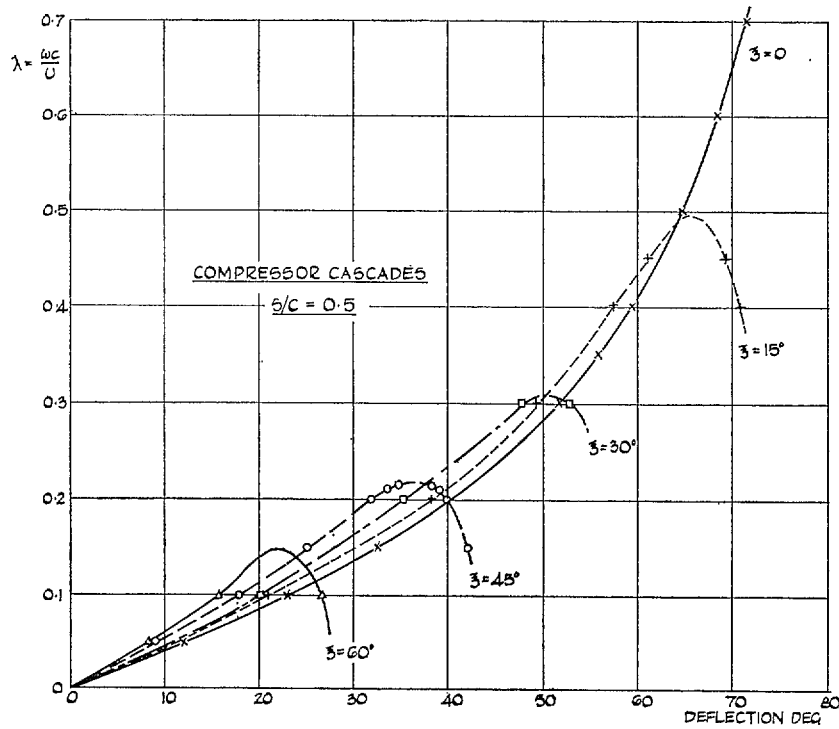
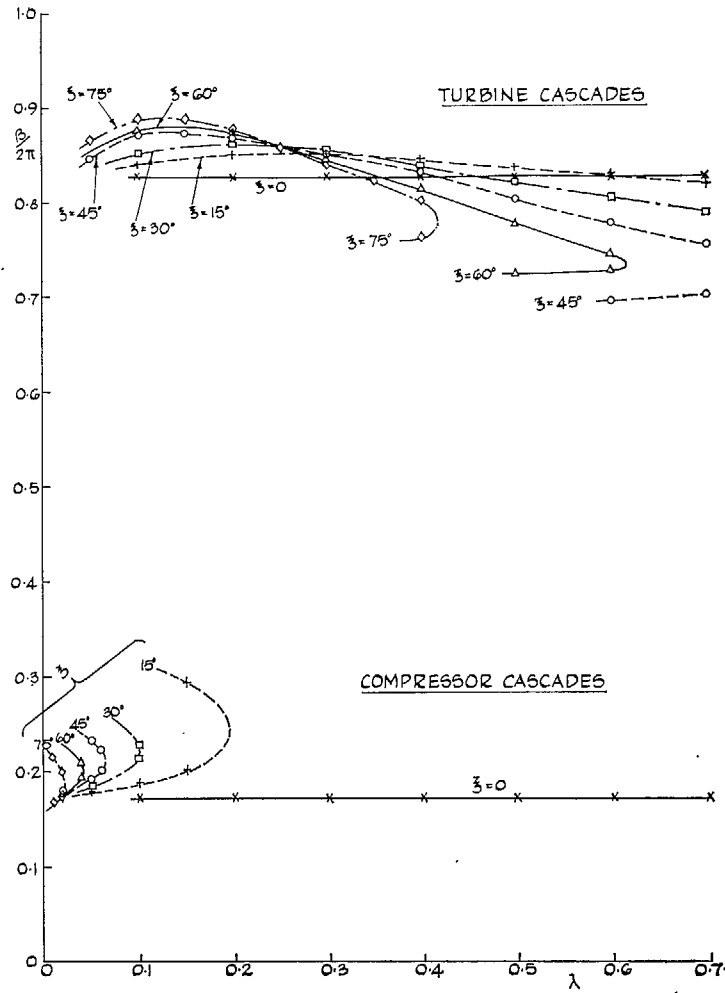
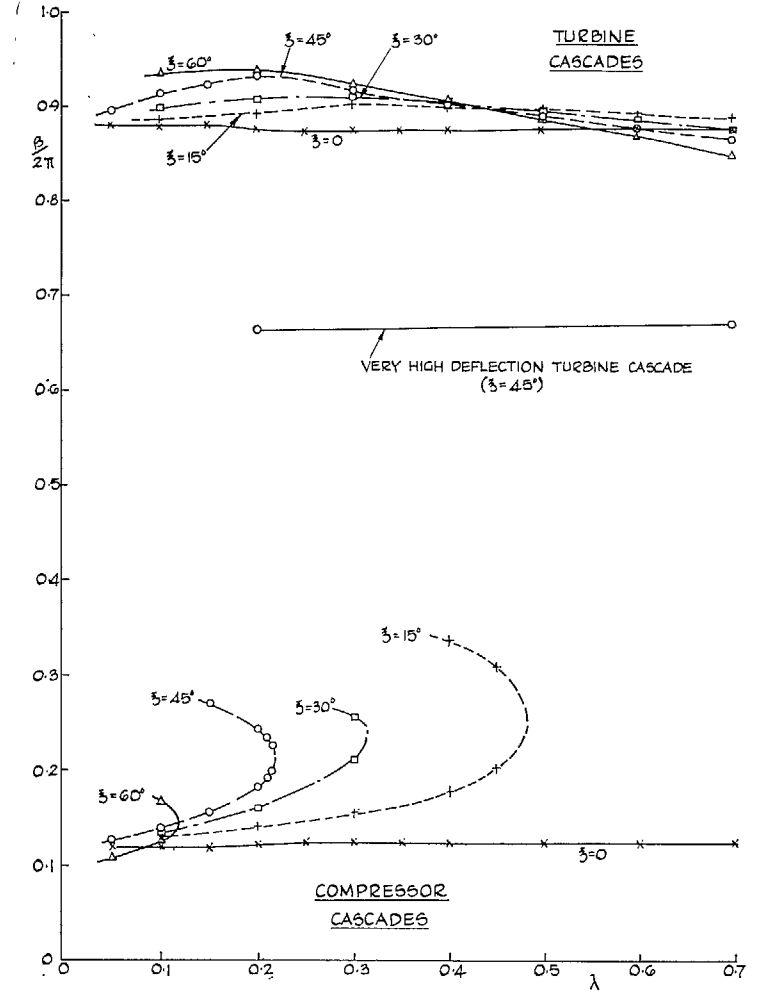


FIG. 13. Critical frequency parameter for flutter.

FIG. 14. Critical phase angle for flutter: $s/c = 1.0$.FIG. 15. Critical phase angle for flutter: $s/c = 0.5$.

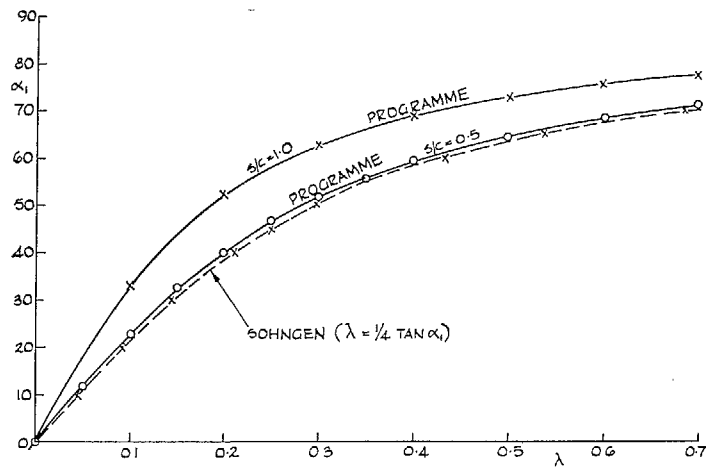


FIG. 16. Comparison with Sohngen's flutter result: $\xi = 0$.

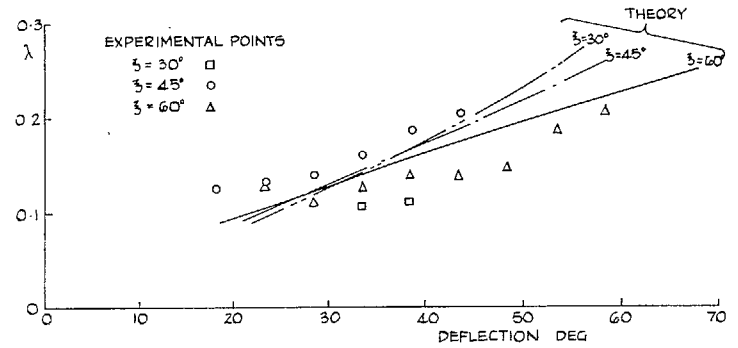


FIG. 17. Comparison with Shioiri's experiment—turbine cascades: $s/c = 0.6$, $\beta/2\pi = 5/6$.

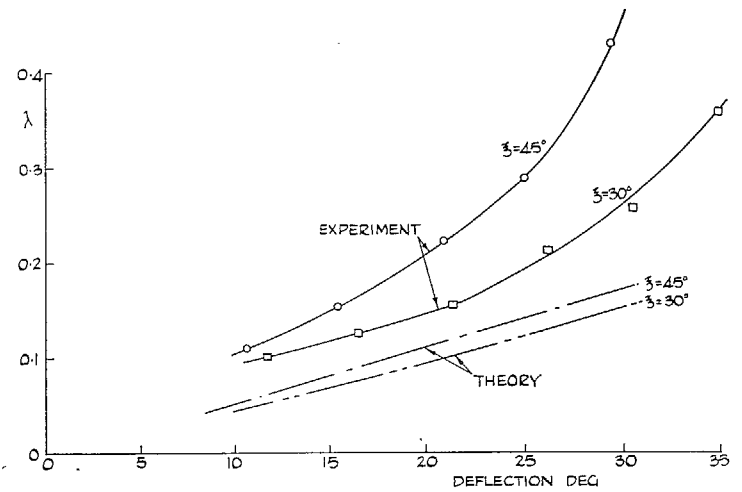


FIG. 18. Comparison with Shioiri's experiment—compressor cascades: $s/c = 0.6$, $\beta/2\pi = 1/6$.

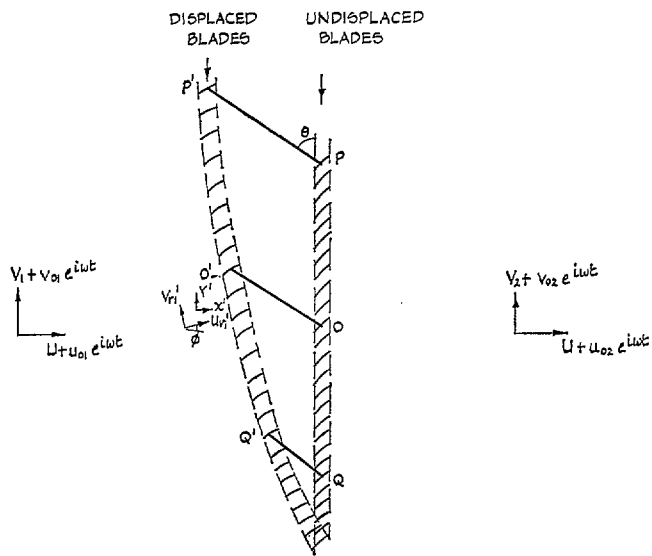


FIG. 19. Diagram for actuator-disc theory.

Publications of the Aeronautical Research Council

ANNUAL TECHNICAL REPORTS OF THE AERONAUTICAL RESEARCH COUNCIL (BOUND VOLUMES)

- 1942 Vol. I. Aero and Hydrodynamics, Aerofoils, Airscrews, Engines. 75s. (post 2s. 9d.)
Vol. II. Noise, Parachutes, Stability and Control, Structures, Vibration, Wind Tunnels. 47s. 6d. (post 2s. 3d.)
- 1943 Vol. I. Aerodynamics, Aerofoils, Airscrews. 80s. (post 2s. 6d.)
Vol. II. Engines, Flutter, Materials, Parachutes, Performance, Stability and Control, Structures. 90s. (post 2s. 9d.)
- 1944 Vol. I. Aero and Hydrodynamics, Aerofoils, Aircraft, Airscrews, Controls. 84s. (post 3s.)
Vol. II. Flutter and Vibration, Materials, Miscellaneous, Navigation, Parachutes, Performance, Plates and Panels, Stability, Structures, Test Equipment, Wind Tunnels. 84s. (post 3s.)
- 1945 Vol. I. Aero and Hydrodynamics, Aerofoils. 130s. (post 3s. 6d.)
Vol. II. Aircraft, Airscrews, Controls. 130s. (post 3s. 6d.)
Vol. III. Flutter and Vibration, Instruments, Miscellaneous, Parachutes, Plates and Panels, Propulsion. 130s. (post 3s. 3d.)
Vol. IV. Stability, Structures, Wind Tunnels, Wind Tunnel Technique. 130s. (post 3s. 3d.)
- 1946 Vol. I. Accidents, Aerodynamics, Aerofoils and Hydrofoils. 168s. (post 3s. 9d.)
Vol. II. Airscrews, Cabin Cooling, Chemical Hazards, Controls, Flames, Flutter, Helicopters, Instruments and Instrumentation, Interference, Jets, Miscellaneous, Parachutes. 168s. (post 3s. 3d.)
Vol. III. Performance, Propulsion, Seaplanes, Stability, Structures, Wind Tunnels. 168s. (post 3s. 6d.)
- 1947 Vol. I. Aerodynamics, Aerofoils, Aircraft. 168s. (post 3s. 9d.)
Vol. II. Airscrews and Rotors, Controls, Flutter, Materials, Miscellaneous, Parachutes, Propulsion, Seaplanes, Stability, Structures, Take-off and Landing. 168s. (post 3s. 9d.)
- 1948 Vol. I. Aerodynamics, Aerofoils, Aircraft, Airscrews, Controls, Flutter and Vibration, Helicopters, Instruments, Propulsion, Seaplane, Stability, Structures, Wind Tunnels. 130s. (post 3s. 3d.)
Vol. II. Aerodynamics, Aerofoils, Aircraft, Airscrews, Controls, Flutter and Vibration, Helicopters, Instruments, Propulsion, Seaplane, Stability, Structures, Wind Tunnels. 110s. (post 3s. 3d.)

Special Volumes

- Vol. I. Aero and Hydrodynamics, Aerofoils, Controls, Flutter, Kites, Parachutes, Performance, Propulsion, Stability. 126s. (post 3s.)
- Vol. II. Aero and Hydrodynamics, Aerofoils, Airscrews, Controls, Flutter, Materials, Miscellaneous, Parachutes, Propulsion, Stability, Structures. 147s. (post 3s.)
- Vol. III. Aero and Hydrodynamics, Aerofoils, Airscrews, Controls, Flutter, Kites, Miscellaneous, Parachutes, Propulsion, Seaplanes, Stability, Structures, Test Equipment. 189s. (post 3s. 9d.)

Reviews of the Aeronautical Research Council

1939-48 3s. (post 6d.)

1949-54 5s. (post 5d.)

Index to all Reports and Memoranda published in the Annual Technical Reports

1909-1947

R. & M. 2600 (out of print)

Indexes to the Reports and Memoranda of the Aeronautical Research Council

Between Nos. 2351-2449

R. & M. No. 2450 2s. (post 3d.)

Between Nos. 2451-2549

R. & M. No. 2550 2s. 6d. (post 3d.)

Between Nos. 2551-2649

R. & M. No. 2650 2s. 6d. (post 3d.)

Between Nos. 2651-2749

R. & M. No. 2750 2s. 6d. (post 3d.)

Between Nos. 2751-2849

R. & M. No. 2850 2s. 6d. (post 3d.)

Between Nos. 2851-2949

R. & M. No. 2950 3s. (post 3d.)

Between Nos. 2951-3049

R. & M. No. 3050 3s. 6d. (post 3d.)

Between Nos. 3051-3149

R. & M. No. 3150 3s. 6d. (post 3d.)

HER MAJESTY'S STATIONERY OFFICE

from the addresses overleaf

© *Crown copyright* 1965

Printed and published by
HER MAJESTY'S STATIONERY OFFICE

To be purchased from
York House, Kingsway, London W.C.2
423 Oxford Street, London W.1
13A Castle Street, Edinburgh 2
109 St. Mary Street, Cardiff
39 King Street, Manchester 2
50 Fairfax Street, Bristol 1
35 Smallbrook, Ringway, Birmingham 5
80 Chichester Street, Belfast 1
or through any bookseller

Printed in England